Journal of Prosthodontics and Implantology

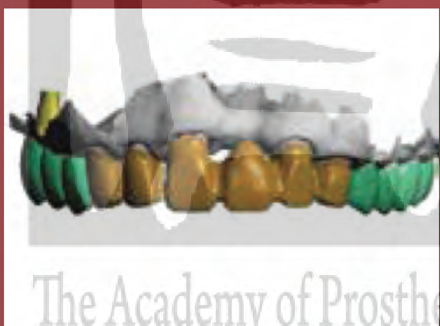

CAD file after virtual cutback, prior to milling, Page 19 Fig. 15

The geometric model is imported to FEM software, Page 28 Fig. 3

Official Journal of
The Academy of Prosthetic Dentistry, R.O.C., Taiwan

Volume 7 Number 4
December 2018

The Academy of Prosthetic Dentistry R.O.C., Taiwan

Journal of Prosthodontics and Implantology

中華民國贗復牙科學會期刊

Vol.7, No.4 December 2018

Subscription ：USD $100/ year　訂價年費： NT $3000 （四期）

創刊日期 ：2012年4月

出版者 ：中華民國贗復牙科學會　學會地址：105台北市復興北路465號2樓　學會電話：+886-2-2546-8834

學會傳真： +886-2-2546-9157　學會官網： http://www.prosthod.org.tw

ISSN 2304-5418

承製編印：美艾聯和股份有限公司　地址：235 新北市新店區中央四街91號　電話：+886-2-2219-4719

Table of Contents

Editorial

Greetings to the 30th anniversary of the Academy of Prosthetic Dentistry, R.O.C. The glory of self-improvement in efforts, wisdom, and expectations of all prosthodontists, furthermore with strong faith and pride accomplishes tremendous growing developments over the 30 years. As the founder member, I am honored to be the committee member and dedicate my best to the Academy.

There are no short cuts to success. It accumulates in the result of preparations, hard work, and learning from failure. Review the past helps one to understand the present. In this volume, three cases and two studies are deliberated. Within case reports, experiences may improve judgments. In place of studies, findings from experiences can assemble such measures and be attainable to dental practices. These articles are worth your reading and I am pleased to share this issue with you. At last, great appreciation to all participants and we look forward to more distinct articles that may be beneficial to all prosthodontists in the future.

Hsiu - Na Lin

Hsiu-Na Lin
Editor-in-Chief

The Academy of Prosthetic Dentistry R.O.C., Taiwan

Case Report

Computer-Guided Immediate Implant Placement And Provisionalization with Definitive CAD/CAM Abutment: A Case Report

Hung-Yuan Lee, DDS
Chief Resident Doctor, Department of Dentistry, Shin Kong Wu Ho-Su Memorial Hospital, Taipei, Taiwan

Chieh-Ming Yu, DDS
Attending Doctor, Department of Dentistry, Shin Kong Wu Ho-Su Memorial Hospital, Taipei, Taiwan

Hsiao-Lin Wu, CDT
Dental Technician, Department of Dentistry, Shin Kong Wu Ho-Su Memorial Hospital, Taipei, Taiwan

Ching-Po Hsueh, DDS
Resident Doctor, Department of Dentistry, Shin Kong Wu Ho-Su Memorial Hospital, Taipei, Taiwan

Chia-Cheng Lin DDS, MBA
Attending Doctor, Department of Dentistry, Shin Kong Wu Ho-Su Memorial Hospital, Taipei, Taiwan
Assistant Professor, School of Dental Technology, College of Oral Medicine, Taipei Medical University

Corresponding author:
Chia-Cheng Lin, DDS, MBA
Attending Doctor, Department of Dentistry, Shin Kong Wu Ho-Su Memorial Hospital, Taipei, Taiwan
Assistant Professor, School of Dental Technology, College of Oral Medicine, Taipei Medical University
No.95, Wen-Chang Rd, Shih Lin District, Taipei, 111, Taiwan, R.O.C.
Tel: +886-2-2833-2211#2181
E-mail: m000703@ms.skh.org.tw

DOI: 10.6926/JPI.201812_7(4).0001

Abstract

Immediate provisionalization with definitive customized abutment is beneficial for maintenance of the marginal bone and surrounding gingival tissue. To fabricate the definitive customized abutment before implant surgery, however, is of considerable uncertainty because it is difficult to place the implant exactly in the position and angulation as planned. This report describes a case in which computer-guided immediate implant placement and provisionalization with definitive CAD/CAM abutment was applied with a stereolithographic surgical guide. Due to the relatively proper implant position provided by this approach, the treatment process proceeded relatively smoothly, and the clinical outcomes with regard to esthetics and function were satisfactory. The technique used saved a lot of chair time, and the postsurgical discomfort of the patient was extremely low; therefore, implementation of the technique in similar clinical situations may well be appropriate.

Key words: Computer-guided surgery, Computer-aided design, Computer-aided manufacturing, Immediate dental implant, Stereolithographic surgical guide

Introduction

The procedure for flapless immediate implant placement in a fresh extraction socket with bare hands is difficult in terms of controlling the axis and depth of the implant[1, 2]. The vibrations and slippage that may occur when drilling an uneven surface of the extraction socket often cause the placement of the implant to deviate from the intended placement[3, 4]. To reduce the trauma inflicted on the patient and achieve an ideal implant position, the operator must be highly experienced, well-trained, and have excellent surgical skills[1, 2, 5, 6].

Immediate provisionalization with definitive customized abutment and implant placement right after tooth extraction can support the surrounding gingival tissue and thus prevent its collapse. This approach also simplifies the complex prosthetic procedure of making the final restoration. In contrast, when a temporary abutment is used to support the provisional crown, it must be repeatedly removed and reinstalled during the fabrication of the final crown, and this may undermine the healing of epithelial tissue and result in gingival recession and other complications[7]. However, it is

Fig. 1: Left maxillary central incisor horizontal fracture.

Fig. 2: Intraoral scanning image (left and middle) of the temporary restoration.

difficult to fabricate an appropriate definitive customized abutment for immediate implant placement in a fresh extraction socket before implant surgery due to difficulty in placing the implant with the precise positioning and angulation planned. The position of the implant shoulder and the distance between the implant and the surrounding gingiva can vary from the expected position, making the prefabricated definitive customized abutment unusable or unfavorable in terms of the margin location and abutment configuration.

This report describes a case in which computer-guided immediate implant placement was applied with a stereolithographic surgical guide. Employing a complete digital workflow, a CAD/CAM definitive abutment and a provisional crown were prefabricated according to the virtual implant treatment planning. With the assistance of the computer surgical guide, the implant was placed close to the planned position. Due to the relatively proper implant position provided by this approach, the treatment process proceeded relatively smoothly, and the clinical outcomes with regard to esthetics and function were good.

Case Report

A 42-year-old woman came to the department of dentistry in Shin Kong Wu Ho-Su Memorial Hospital complaining of a fracture to her left maxillary central incisor due to traumatic injury (Fig. 1). The tooth had previously undergone a root canal treatment and a crown restoration many years before. The patient claimed neither major systemic diseases nor allergies. She wanted to extract the retained root because she did not wish to undergo any complicated treatment procedures. Since she wanted to have dental implant treatment after extraction of the root, immediate implant placement, and provisionalization was suggested and accepted.

A temporary restoration was fabricated with fiber post and resin composite on the root for esthetic purposes. Using a large field-of-view CBCT scanner (KaVo 3D eXam, KaVo Dental, Biberach, Germany), 3-dimensional radiographic images were obtained for preoperative assessment of the alveolar bone. Using an intraoral scanner (3Shape TRIOS® 3, Copenhagen, Denmark), maxillary and mandibular digital impressions and the interocclusal registration were acquired (Fig. 2). These two forms of digital data were then imported into an implant planning software program (BenQ AB guided Service, Ashdod, Israel) and aligned. Once the alignment was verified, the surgeon could then develop a virtual implant treatment plan with the software. Considering the ideal restoration morphology and the anatomical condition of the patient, a virtual implant with proper diameter and length was designed using the implant planning software.

According to the virtual implant treatment

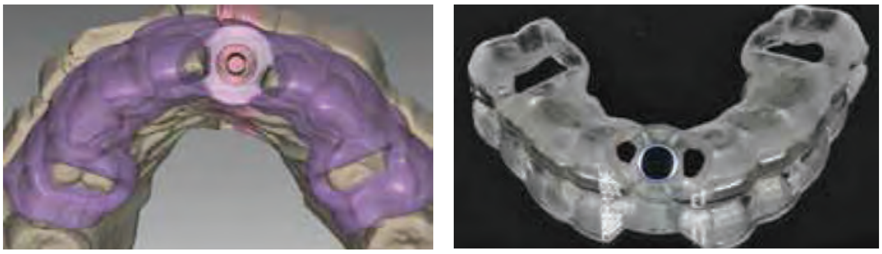

Fig. 3: Design and production of the stereolithographic surgical guide.

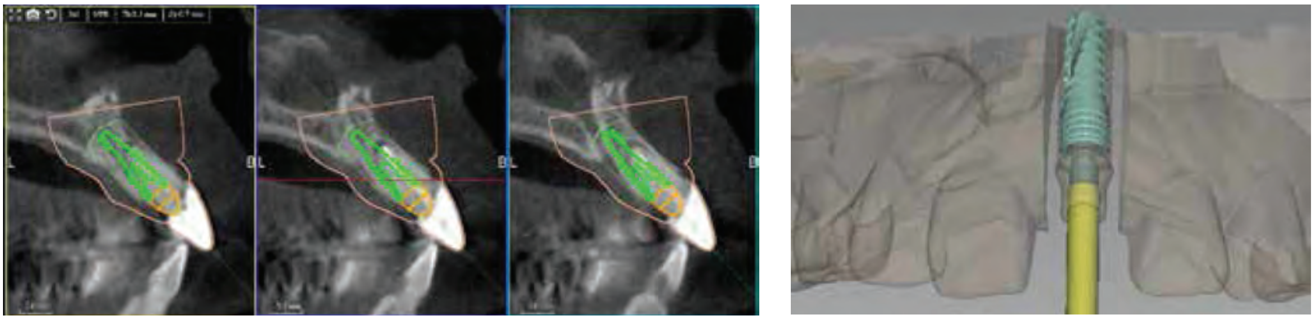

Fig. 4 : Determined virtual implant position sent to dental CAD software.

Fig. 5 : CAD/CAM production of the definitive titanium abutment and the polymethyl methacrylate-based temporary crown.

Fig. 6 : Immediate implant placement via stereolithographic surgical guide.

plan, a stereolithographic surgical guide (BenQ AB Guide, Taipei, Taiwan) was fabricated (Fig. 3). The determined virtual implant position was then sent to a dental CAD software program (Exocad Dental CAD, Darmstadt, Germany) (Fig. 4). With this software, the dental technician designed an abutment and a provisional crown conforming to the virtual implant position and its surrounding gingival tissue, after which the definitive titanium abutment and the polymethyl methacrylate-based temporary crown were fabricated using the CAM milling process (Fig.5) and prepared for the surgery.

After atraumatic extraction of the retained root, the tooth-supported stereolithographic surgical guide was verified in the patient's mouth for the seating position and stability. An osteotomy was performed following the drilling protocol of the surgical guide, then a pre-planned 4.2x13 mm implant (AB Dental, Ashdod, Israel) was immediately placed via the surgical guide (Fig. 6). After good primary stability (over 35N/cm) was achieved and confirmed, the customized definitive titanium abutment was connected to the implant after filling the gap between the implant and extraction socket with alloplastic grafting material (SinBoneHT, Purzer Pharmaceutical, Taipei, Taiwan). Due to the relatively proper implant position, the CAD/CAM abutment was well fitted, with only the finishing line of the buccal margin requiring some adjustment (Fig. 7). The provisional crown was then relined and set on the abutment with temporary cement. All the centric and eccentric occlusal contacts were removed to prevent overloading on the implant (Fig. 8).

Fig. 7 : After some adjustment of the buccal surface and finishing line, the definitive titanium abutment was placed on the implant.

Fig. 8 : Provisional crown was relined and set on the abutment.

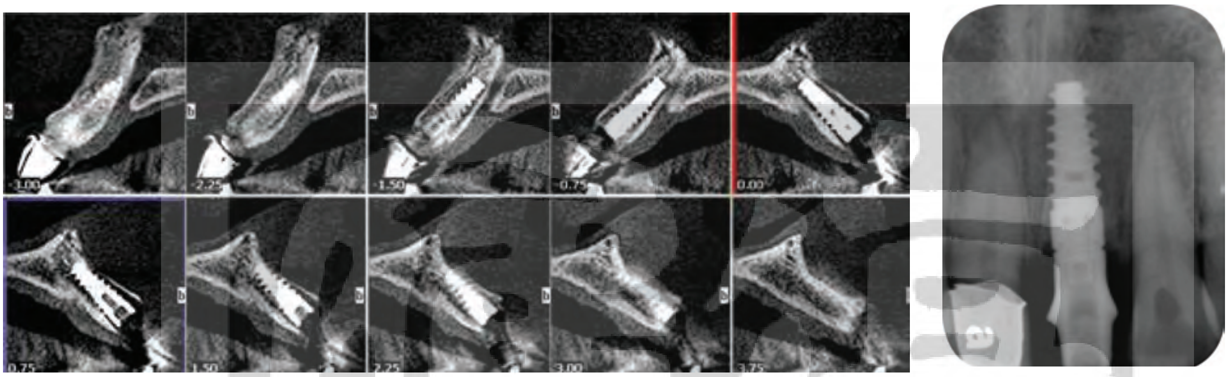

Fig. 9 : Post-operative CBCT and the periapical film showed that the implant was placed very close to the planned position, with slight buccal deviation.

With the approval of the hospital's ethics committee, the corresponding author of this report was conducting a clinical research study regarding the accuracy of implant positioning with the stereolithographic surgical guide. The patient agreed to enroll in the study, so a post-operative CBCT image and periapical film were taken (Fig. 9). The radiographs showed that the implant was placed very close to the planned position, with only slight buccal deviation. One day after the surgery, the wound exhibited good healing (Fig. 10), and the patient complained of neither pain nor swelling. At the two-month follow-up appointment, the buccal margin of the abutment was modified again and the provisional crown was relined for the remodeling of the gingival tissue. Six months after the implant placement, the gingival tissue showed excellent remodeling (Fig. 11), and a zirconia crown was fabricated using the conventional impression method without taking out the abutment. At the two-year follow-up appointment, the implant restoration exhibited satisfying outcomes in terms of esthetics and function (Fig. 12).

Discussion

Because it can be easily adjusted to match the gingival height and contour after implant placement, a provisional abutment is usually utilized for an immediately placed anterior implant. However, to fabricate the final restoration after osseointegration of the implant, such a provisional abutment would have to be removed and reinstalled several times during the prosthetic procedure. This repeated abutment removal could lead to more bone loss than would be seen with the use of a non-removable abutment[8, 9]. A definitive, non-removable abutment is therefore beneficial for the maintenance of the marginal bone and the surrounding gingival tissue, especially for thin-biotype patients. Moreover, a digitally designed and milled definitive abutment mimicking the root shape of the extracted tooth can be effectively molded to the peri-implant soft tissue to duplicate the gingival contour of the natural tooth. However, unless the surgeon can insert the implant properly in the planned position, using definitive customized abutments in such situations is very challenging. Any substantial angular or spatial deviation of

Fig. 10: The next day after surgery. Healing was good, neither pain nor swelling complained.

Fig. 11: Six-month recall. Modified provisional crown with excellent gingival remodeling.

Fig. 12 : Two-year recall. Satisfying outcome regarding esthetics and function.

the inserted implant would necessitate extensive modification of the abutment in order to fit the abutment into the proper position.

One of the advantages of computer-guided implant surgery is the accuracy of the implant position in comparison to that achieved with non-guided surgery[10]. In a systematic review regarding the accuracy of static computer-guided implant surgery published by Van Assche et al.[11], an overall mean deviation of 0.99 mm at the entry point (standard error: 0.12 mm; range: 0–6.5 mm) and a mean angular deviation of 3.81 degrees (standard error: 0.32°, range: 0–24.9°) were reported. Those authors concluded that the accuracy of computer-guided implant placement was significantly better than that of non-guided implant placement (that is, guided drilling with free-hand implant placement), a finding which was also reported in other review papers[12-14]. In the case reported herein, computer-guided implant placement in a fresh extraction socket with a stereolithographic surgical guide was utilized. The surgical guide not only helped to prevent the drilling direction from deviating to the extraction socket but also helped to place the implant correctly in the planned position. Thus, the prefabricated definitive abutment could be effectively applied in the immediate restoration procedure.

Although the mean deviation of static computer-guided implant placement has been found to be reasonably low, relatively high maximum deviations have been reported in the literature[15]. Testori et al.[16] suggested that a safe distance of at least 2 mm is needed between implants and anatomic structures when planning computer-guided implant surgery. With the consent of the patient and the approval of the ethical committee, the deviations between the planned and real implant positions for the case reported herein were analyzed by overlapping the digital treatment plan and the post-operative CBCT data (Fig. 13). The horizontal and vertical deviations at the implant shoulder were 0.71 mm and 0.22 mm, respectively, and the angular deviation was 2.92 degrees. The deviation analysis resulting from the overlapping with the CBCT data could have potential errors due to the inaccuracies in the CBCT scan reconstruction and the interference of metallic streaking artifacts. Nevertheless, the analytic measuring method used in this report was consistent with the method used in other studies, so the results of this report could still be useful as references. It seems that the deviations in this case were comparable with the mean value derived from the other studies of computer-guided implant placement.

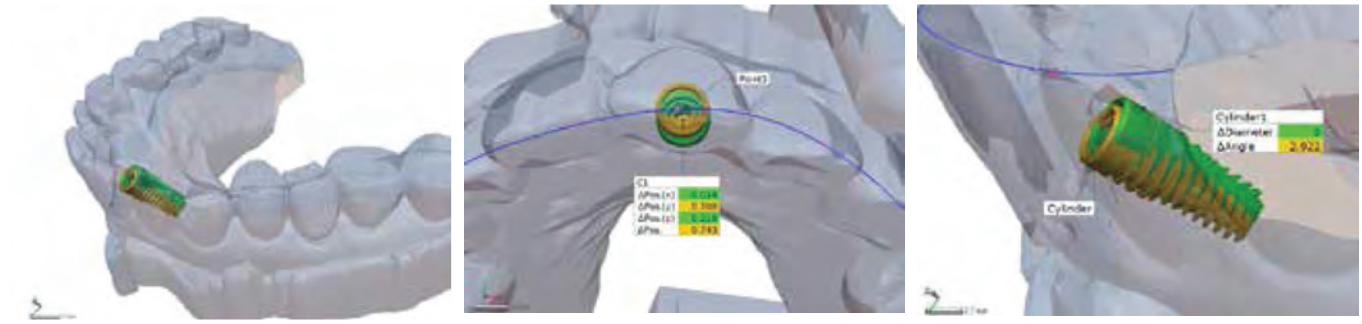

Fig. 13: Deviations between the planned and real implant position were analyzed by overlapping the digital treatment plan and the post-operative CBCT data.

At present, from the acquisition of the patient's clinical data to the execution of the guided surgery, computer-guided implant placement via stereolithographic surgical guide remains a complicated procedure involving many steps[13]. The quality of the CBCT images and the digital model, the registration of the CBCT data and model surface scan[17], the precision of the surgical guide production, the mechanical tolerance between surgical instruments and the surgical guide[18], and the positioning of the surgical guide during implant surgery can all affect the accuracy or inaccuracy of computer-guided implant placement. Initially, a radiographic scan prosthesis was needed to plan the computer guide using the so-called "double scan" or "dual scan" technique[13]. Nowadays, a new technique is advocated in which a CBCT scan is mapped with the optical scan of the dental cast in partially edentulous patients. Errors resulting from the fabrication and scanning of a radiographic scan prosthesis can be avoided in this technique[19]. The case reported herein also implemented this new technique, except that an intraoral scan instead of a dental cast scan was used in the computer planning procedure. This digital work-flow is probably more accurate in addition to being cost- and time-saving[20]. Further studies are needed, however, to examine the accuracy of guided implant surgery based on matching the CBCT scan with the intraoral scan.

In this case report, the implant deviated mainly to the buccal side. Although the sleeve of the surgical guide had confined the implant direction during the implant placement, the implant still tended to be driven towards the space of the extraction socket. A surgeon should thus always keep in mind that great deviations of the implant could still occur even with the help of the computer surgical guide. Nonetheless, this report presents a technique that saved a lot of chair time. The clinical outcomes were good, and the postsurgical discomfort of the patient was extremely low; therefore, implementation of the technique in similar clinical situations may well be appropriate.

References

1. Greenstein G, Cavallaro J. Immediate dental implant placement: technique, part I. Dent Today 2014;33(1):98, 100-4; quiz 05.
2. Cavallaro J, Greenstein G. Immediate dental implant placement: technique, part 2. Dent Today 2014;33(2):94, 96-8; quiz 99.
3. Al-Sabbagh M, Kutkut A. Immediate implant placement: surgical techniques for prevention and management of complications. Dent Clin North Am 2015;59(1):73-95.
4. Al-Sabbagh M. Implants in the esthetic zone. Dent Clin North Am 2006;50(3):391-407, vi.
5. Guarnieri R, Ceccherini A, Grande M. Single-tooth replacement in the anterior maxilla by means of immediate implantation and early loading: clinical and aesthetic results at 5 years. Clin Implant Dent Relat Res 2015;17(2):314-26.
6. Cannizzaro G, Leone M, Ferri V, et al. Immediate loading of single implants inserted flapless with medium or high insertion torque: a 6-month follow-up of a split-mouth randomised controlled trial. Eur J Oral Implantol 2012;5(4):333-42.
7. Abrahamsson I, Berglundh T, Sekino S, Lindhe J. Tissue reactions to abutment shift: an experimental study in dogs. Clin Implant Dent Relat Res 2003;5(2):82-8.
8. Grandi T, Guazzi P, Samarani R, Maghaireh H, Grandi G. One abutment-one time versus a provisional abutment in immediately loaded post-extractive single implants: a 1-year follow-up of a multicenter randomised controlled trial. Eur J Oral Implantol 2014;7(2):141-9.
9. Degidi M, Nardi D, Piattelli A. One abutment at one time: non-removal of an immediate abutment and its effect on bone healing around subcrestal tapered implants. Clin Oral Implants Res 2011;22(11):1303-7.
10. Vercruyssen M, Hultin M, Van Assche N, et al. Guided surgery: accuracy and efficacy. Periodontology 2000 2014;66(1):228-46.
11. Van Assche N, Vercruyssen M, Coucke W, et al. Accuracy of computer-aided implant placement. Clin Oral Implants Res 2012;23 Suppl 6:112-23.
12. Zhou W, Liu Z, Song L, Kuo CL, Shafer DM. Clinical Factors Affecting the Accuracy of Guided Implant Surgery-A Systematic Review and Meta-analysis. J Evid Based Dent Pract 2018;18(1):28-40.
13. Vercruyssen M, Laleman I, Jacobs R, Quirynen M. Computer-supported implant planning and guided surgery: a narrative review. Clin Oral Implants Res 2015;26 Suppl 11:69-76.
14. Tahmaseb A, Wismeijer D, Coucke W, Derksen W. Computer technology applications in surgical implant dentistry: a systematic review. Int J Oral Maxillofac Implants 2014;29 Suppl:25-42.
15. Schneider D, Marquardt P, Zwahlen M, Jung RE. A systematic review on the accuracy and the clinical outcome of computer-guided template-based implant dentistry. Clin Oral Implants Res 2009;20 Suppl 4:73-86.
16. Testori T, Robiony M, Parenti A, et al. Evaluation of accuracy and precision of a new guided surgery system: a multicenter clinical study. Int J Periodontics Restorative Dent 2014;34 Suppl 3:s59-69.
17. Flugge T, Derksen W, Te Poel J, et al. Registration of cone beam computed tomography data and intraoral surface scans - A prerequisite for guided implant surgery with CAD/CAM drilling guides. Clin Oral Implants Res 2017;28(9):1113-18.
18. Casse_a M, Di Mambro A, Di Giorgio G, Stefanelli LV, Barbato E. The Influence of the Tolerance between Mechanical Components on the Accuracy of Implants Inserted with a Stereolithographic Surgical Guide: A Retrospective Clinical Study. Clin Implant Dent Relat Res 2015;17(3):580-8.
19. Widmann G, Berggren JP, Fischer B, et al. Accuracy of Image-Fusion Stereolithographic Guides: Mapping CT Data with Three-Dimensional Optical Surface Scanning. Clin Implant Dent Relat Res 2015;17 Suppl 2:e736-44.
20. Arunyanak SP, Harris BT, Grant GT, Morton D, Lin WS. Digital approach to planning computer-guided surgery and immediate provisionalization in a partially edentulous patient. J Prosthet Dent 2016;116(1):8-14.

Case Report

Prosthetic Rehabilitation with Root And Implant-Retained Maxillary Overdentures: A Clinical Report

Tsung-Kai Chang, DDS
Taipei MacKay Memorial Hospital, Taipei, Taiwan

Corresponding author:

Tsung-Kai Chang, DDS
Taipei MacKay Memorial Hospital, Taipei, Taiwan
No. 92, Sec. 2, Zhongshan N. Rd., Taipei City 10449, Taiwan, R.O.C.
Tel: 886-2-2543-3535 ext. 2216
Fax: 886-2-2543-3642
E-mail: mascot1110@hotmail.com

DOI: 10.6926/JPI.201812_7(4).0002

Abstract

Overdentures have been used as dental prostheses for many years. Compared with conventional complete dentures, overdentures can preserve a patient's roots or rely on implants for vertical support, and overdentures also have many other advantages, such as maintaining the height of the ridge while also improving retention and chewing performance. Moreover, rather than requiring the extraction of all compromised teeth, overdentures allow the roots or even previous malpositioned implants to be utilized as overdenture abutments. When used in conjunction with attachments, overdentures can also provide better retention and stability than conventional dentures.

The purposes of this clinical report are to present how full mouth rehabilitation can be implemented through the use of implants and a root as maxillary overdenture abutments and to discuss the previous literature related to the treatment described.

Key words: Dental implant, implant-retained overdenture, locator attachment, overdenture

Introduction

The full mouth rehabilitation of patients with generalized periodontitis is challenging for clinicians in terms of deciding whether or not the teeth can be preserved. If the prognosis for the remaining teeth is poor, an overdenture may be a good treatment when applied in conjunction with the extraction of the hopeless teeth and the preservation of some roots as overdenture abutments.

Alveolar bone is resorbed when teeth are extracted. The function of complete dentures is thus not as effective as that of natural teeth due to the resulting lack of occlusal support. Overdentures offer a solution by retaining natural teeth for vertical support. By the 1960s, a considerable amount of information regarding whether the concept of overdentures could provide a workable treatment had been collected. In addition, numerous textbooks have described the specific concepts and methods of overdenture therapy[1].

The purpose of this clinical report is to present how to perform prosthetic rehabilitation through the use of an overdenture in conjunction with the use of a root and two dental implants as abutments combined with

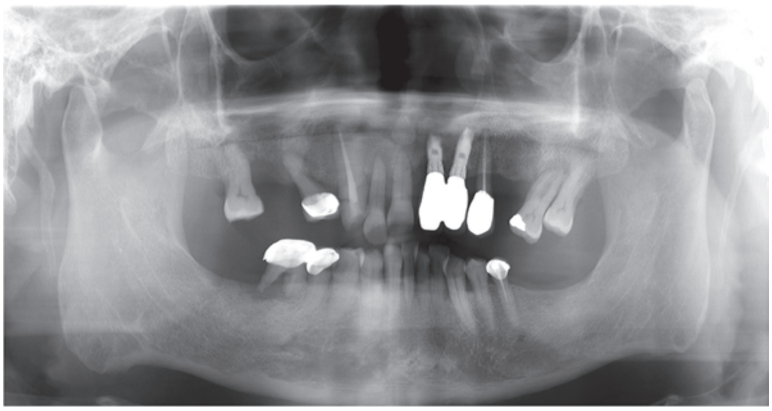

Fig. 1: A panoramic radiograph showing moderate to severe horizontal bone loss, as well as two old dental implants over the anterior maxillary area.

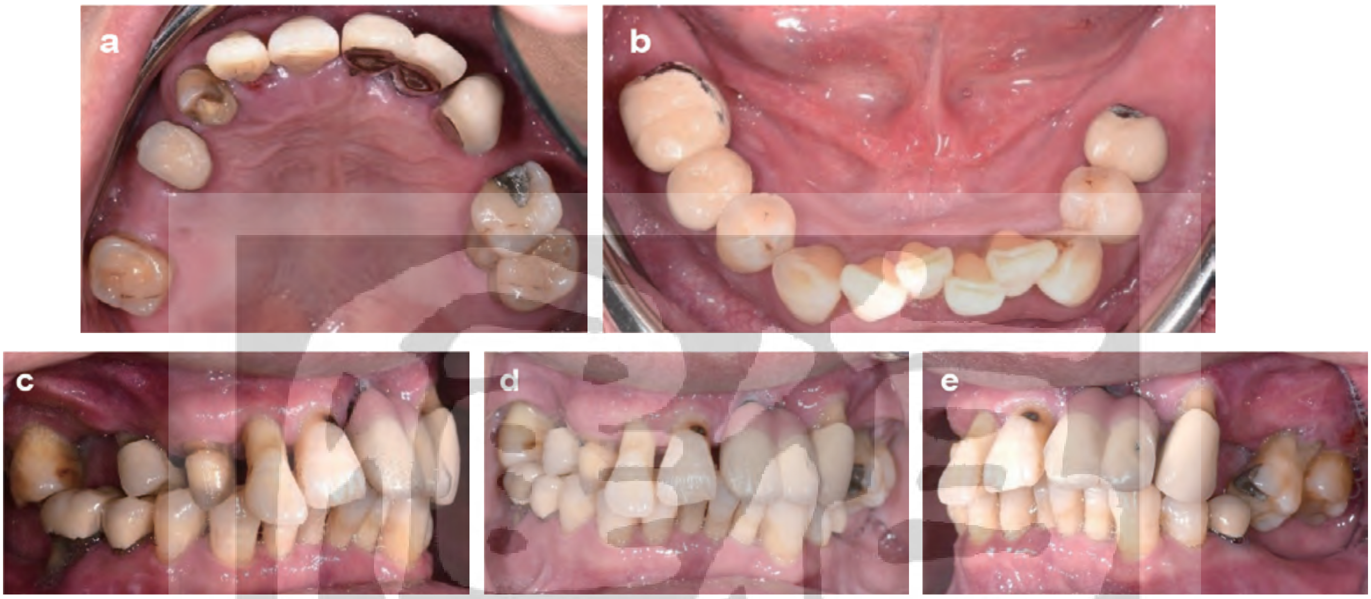

Fig. 2: (a) Occlusal view of the maxillary arch. (b) Occlusal view of the mandibular arch showing tooth crowding. (c) Right-side view revealing the prepared canine and severe bony destruction of the mandibular molar. (d) Frontal view showing greater gingival recession and flare-out of the maxillary anterior teeth. (e) Left-side view showing tilting and downgrowth of the maxillary molars.

two Locator attachments (Zest Anchors, Inc., Escondido, CA, USA).

Case report

A 57-year-old male was suffering from severe periodontitis. The patient came to the periodontal department of Taipei MacKay Memorial Hospital (Taipei, Taiwan) for help. After an initial evaluation, the patient was referred to the prosthodontic department for full mouth rehabilitation. The patient's chief complaints were an unpleasing profile and the loosening of the teeth. The patient's major systemic disease was well-controlled hypertension. The patient denied any drug allergies. An examination revealed that the patient had moderate to severe horizontal bone loss and two previous implants over the upper left central incisor and lateral incisor (Fig. 1). Gingival recession and the flaring out of the anterior teeth were also noted, as was severe bony destruction around the tilting posterior teeth (Fig. 2). Following this survey, the dental problems requiring a solution were listed as follows: ill-fitting old prostheses, unfavorable implant positions, an uneven occlusal plane, and insufficient posterior support.

The initial treatment plan was to control the inflammation, stabilize the occlusion, enhance the chewing function, and regain the esthetics. The first therapies included oral hygiene instructions, the replacement of the old prostheses with provisional crowns, the extraction of hopeless teeth, and nonsurgical periodontal treatment (Fig. 3). Then, an interim overdenture utilizing the maxillary right canine and anterior left implants as abutments for the maxillary arch and a Kennedy Class I interim denture for the mandibular arch were fabricated to reconstruct

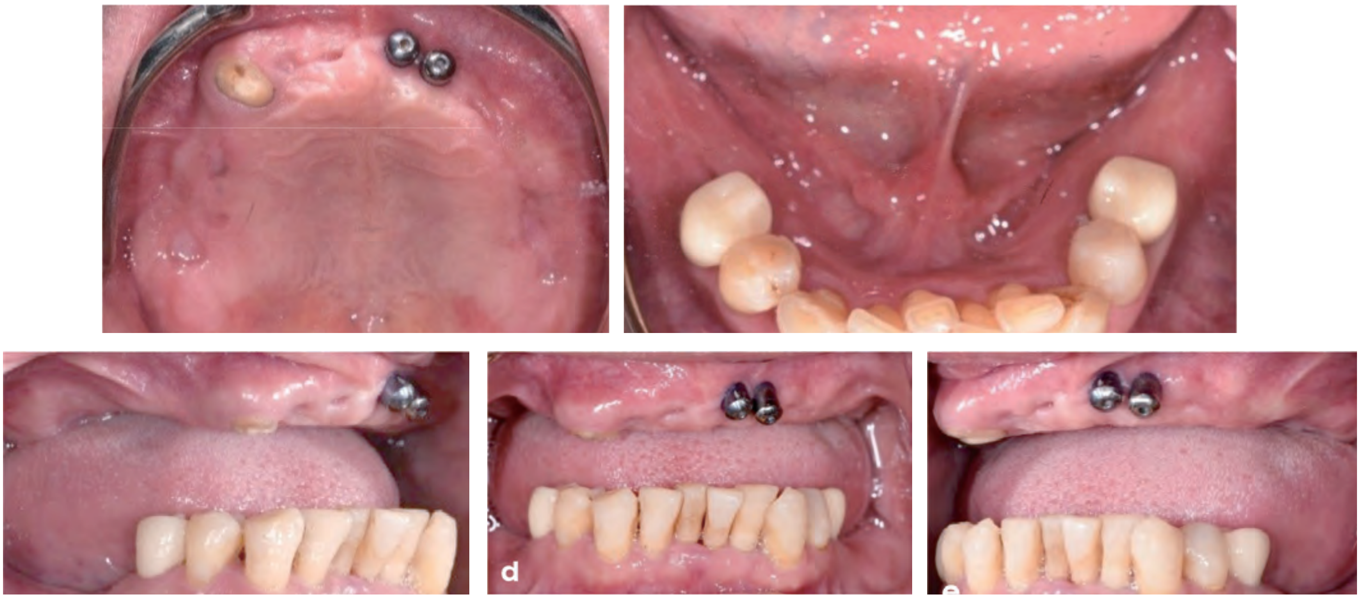

Fig. 3: After extraction, (a) Occlusal view of the maxillary arch. (b) Occlusal view of the mandibular arch. (c) Right-side view. (d) Frontal view. (e) Left-side view.

Fig. 4: Frontal and lateral views of the interim prostheses at the time of delivery. Even occlusal contacts and minimum anterior contact were designed for this case.

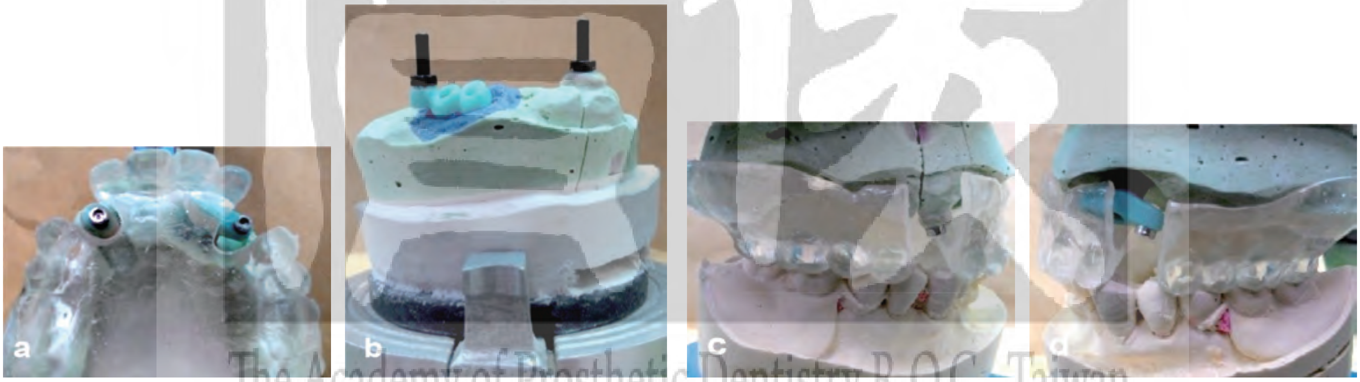

Fig. 5: Wax-up to check the Locator positions (a), parallel condition (b), and restorative space (c and d).

the function and esthetics of the patient (Fig. 4).

After 3 months of follow-up, the patient was satisfied with his chewing capacity and dental appearance. The patient's periodontal condition had become stable without any deep pockets, and the patient had also accommodated himself to the use of the removable prostheses. Hence, the definitive treatment plan was implemented. This plan included the application of Locator attachments in conjunction with the maxillary right canine and anterior left implants, an overdenture with a metal framework of the maxillary arch, surveying crowns of the mandibular left and right second premolars, and a Kennedy Class I RPD of the mandibular arch.

The design of the Locator attachments for the maxillary right canine was the root-form casting type. In order to equilibrate the angulation of the attachments, a casting bar splinting the two previous implants with the Locator attachments on the distal side was fabricated. A stent duplicated from the upper interim denture was used to check the Locator positions and restorative space. A wax-up was

Fig. 6: Delivery of root-form Locator attachment and bar in conjunction with Locator attachment.

Fig. 7: Delivery of surveying crowns.

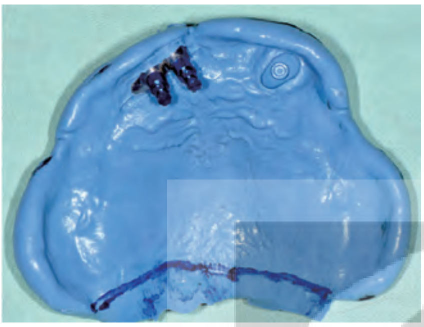

Fig. 8: Maxillary impression made through selective pressure impression.

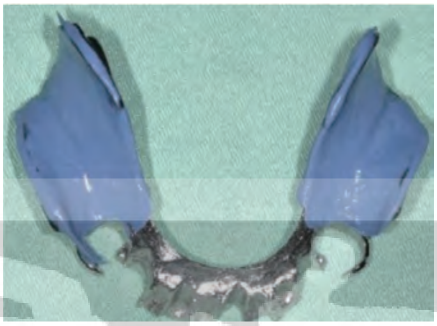

Fig. 9: Altered cast impression used for the free-end area.

Fig. 10: Frontal and lateral views of the final prostheses.

made following this use of the stent (Fig. 5). Then, the Locator attachments were cast and delivered (Fig. 6).

A final impression of the surveying crowns was taken with vinyl polysiloxane impression materials (Panasil® Putty and initial contact X-Light, Kettenbach, Germany). The wax pattern was checked with a surveyor to ensure the appropriate guiding plane and a precise undercut. Metal copings were then fabricated and tried in. The definitive restorations were set with resin cement (RelyX™ U200, 3M ESPE, America) (Fig. 7).

A final impression of the maxillary denture was taken with a custom tray and condensation-type silicone impression materials (Coltex®, COLTENE, Switzerland). The border molding method was implemented to obtain accurate border positions (Fig. 8).

A definitive impression of the Kennedy Class I RPD of the mandibular arch was made with condensation-type silicone impression materials (Coltex®, COLTENE, Switzerland) after surveying, designing, and teeth preparation. In order to make the teeth and the soft tissue support of the denture base as compatible as possible, the altered cast impression technique was executed (Fig. 9).

The occlusal scheme used in this case was bilateral balanced occlusion for the even distribution of occlusal force. The esthetics and bite record were checked with the wax denture. After processing, lab remounting was done to correct the packing error. Finally, the finished prostheses were delivered (Fig. 10).

After the patient wore the new denture for two weeks to let the soft tissue settle

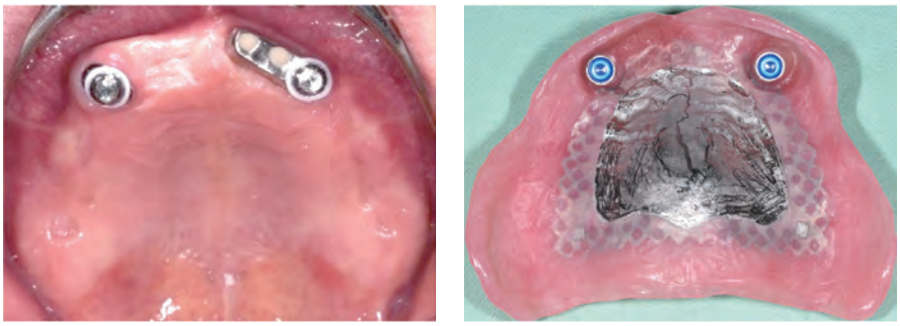

Fig. 11: After the soft tissue settled down, the Locator caps with black processing were intraorally picked up and then changed to the blue male part.

Fig. 12: Instruction in the use of an inter-dental brush for maintenance of oral hygiene.

down, the Locator caps with black processing were intraorally picked up. Then, the blue Locator male retentions were inserted into the denture caps (Fig. 11). The patient was satisfied with the definitive prostheses. The denture was more stable, and the chewing efficiency was improved. A maintenance care program was then performed, including oral hygiene instructions and instructions regarding home care of the denture, especially the use of interdental brushes through the bottom of the bar (Fig. 12). After 12 months of follow-up, no major complications were noticed, and periapical radiography showed that the bone level of the implant was stable (Fig. 13, Fig. 14).

Fig. 13: Periapical radiograph taken after the delivery of the attachments.

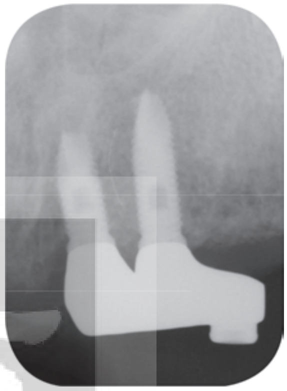

Fig. 14: After 1 year of follow-up, a periapical radiograph showing that the bone level of the implant was stable.

Discussion

Overdentures can be a better treatment option than complete dentures in some cases. As Fenton summarized, overdentures can successfully keep patients from becoming fully edentulous[1]. Through the preservation of the teeth or roots, patients can chew better, maintain their ridge heights, and have dentures that are more stable and retentive. In this case, the patient felt satisfied with the new prostheses due to the improved chewing efficiency they provided.

After the introduction of osseointegrated implants, the possibilities of treatment were notably improved[2]. In the case described above, the overdenture not only used a root but also previous dental implants as abutments. If the osseointegration of the existing implants was good, the replacement of the previous abutment with a new attachment was feasible.

When root abutments fail, it is usually due to caries and vertical root fractures, especially when the abutments are on the maxilla and the opposing teeth are natural teeth[3]. Therefore, the maintenance of oral hygiene care and fluoride application is important. Routine dental check-ups with radiography are also crucial.

Roots and implants can improve the retention and stability of overdentures through the use of attachments[4]. A variety of attachments can be qualified for use, such as ball attachments, Locator attachments, bar attachments, and even magnets[4,5]. The Locator attachment was introduced in 2001, and was selected in the case presented herein due to a number of advantages, such as the various vertical heights and types available for most implant systems and conditions[5]. In addition, a bar can also be used in conjunction with Locator attachments to correct the angulation of implants. The Locator attachment is self-aligning and has resilient dual retention[5-7]. Cakarer and colleagues[8] reported that the rate of complications associated with Locator attachments is lower than that associated with ball and bar systems. However, the use of a bar design requires prudence due to its bulk and the associated oral hygiene problems[9]. That said, a duplicated interim denture can be used as a guide to prevent such problems. The guide can determine the space available for the bar and any attachments.

Despite having the support from the root and implants in this case, the design of the overdenture was still similar to that of a complete denture, such that the primary stress bearing areas were the hard palate and tuberosity. The primary function of the root and implants was to improve the retention through the Locator attachments. Previous studies have suggested the use of four to six implants splinted with a bar to support maxillary overdentures with palate-less designs[2,10]. Meanwhile, the principle of wide coverage with the denture base should still be obeyed in order to decrease the stress per unit[11].

Combination syndrome should be considered in this case. It is a dental condition that frequently occurs when the maxilla is fully edentulous but anterior teeth remain in the mandible[11,12]. The preservation of healthy roots and implants could prevent this condition. The other way to prevent the condition is to properly design the denture with even distribution of the posterior occlusion and light contact of the anterior teeth[12]. Nevertheless, using a root and implants simultaneously as overdenture abutments in the maxillary arch was an innovative method for prosthodontic treatment. Going forward, periodic attention and maintenance due to the necessity of renewing the retention elements and relining the denture base will be indispensable[7,11].

References

1. Fenton AH. e decade of overdentures: 1970-1980. J Prosthet Dent 1998; 79: 31-6.
2. Carlsson GE. Implant and root supported overdentures - a literature review and some data on bone loss in edentulous jaws. J Adv Prosthodont 2014; 6:245-52.
3. Einger RL, Qian F. Postprocedural problems in an overdenture population: a longitudinal study. J Endod 2004; 30:310-4.
4. Trakas T, Michalakis K, Kang K, Hirayama H. Attachment systems for implant retained overdentures: a literature review. Implant Dent. 2006; 15:24-34.
5. Chikunov I, Doan P, Vahidi F. Implant-retained partial overdenture with resilient attachments. J Prosthodont. 2008; 17:141-8.
6. Evtimovska E, Masri R, Driscoll CF, Romberg E. The change in retentive values of locator attachments and hader clips over time. J Prosthodont. 2009; 18:479-83.
7. Vahidi F, Pinto-Sinai G. Complications associated with implant-retained removable prostheses. Dent Clin North Am. 2015; 59:215-26.
8. Cakarer S, Can T, Yaltirik M, Keskin C. Complications associated with the ball, bar and Locator attachments for implant-supported overdentures. Med Oral Patol Oral Cir Bucal. 2011; 16: e953-9.
9. Waddell JN, Payne AG, Swain MV. Physical and metallurgical considerations of failures of soldered bars in bar attachment systems for implant overdentures: a review of the literature. J Prosthet Dent 2006; 96:283–8.
10. Damghani S, Masri R, Driscoll CF, Romberg E. The effect of number and distribution of unsplinted maxillary implants on the load transfer in implantretained maxillary overdentures: an in vitro study. J Prosthet Dent. 2012; 107:358-65.
11. Kelly E. Changes caused by a mandibular removable partial denture opposing a maxillary complete denture. 1972. J Prosthet Dent. 2003; 90:213-9.
12. Tolstunov L. Combination syndrome: classification and case report. J Oral Implantol 2007; 33:139-51.

Case Report

Full Mouth Rehabilitation with Digital Impression And CAD/CAM Technology: A Clinical Report

Chia-Hao Tu, DDS
Department of Prosthodontics,
Chi Mei Medical Center,
Tainan, Taiwan

Corresponding author:

Jui-Chung Chang D.D.S, M.S.
Director,
Department of Prosthodontics,
Chi Mei Medical Center,
Tainan, Taiwan, R.O.C.
Tel: +886-6-282-8928
E-mail: csg129@gmail.com

DOI: 10.6926/JPI.201812_7(4).0003

Abstract

To restore with fixed prosthesis in full mouth rehabilitation, the chance to achieve a satisfactory impression by a conventional impression technique in one time is rare. Moreover, transferring of patient's well-adapted occlusal scheme from the provisional phase to definitive prostheses may not be easy compared to the digital workflow. In the case report presented herein, a digital method and digital reference models were used to take the final impressions, after which full mouth zirconia-based FDPs were fabricated with CAD/CAM technology combined with porcelain layering on anterior teeth.

Key words: CAD/CAM, digital impression, monolithic, zirconia

Introduction

The ongoing advances in digital technology and dental processing have expanded the possibilities in the field of fixed prosthodontics.

Traditionally, the process of manufacturing metal or porcelainfused-to-metal restorations required first taking conventional impressions and pouring stone casts, followed by the completion of wax-up and casting procedures. However, recent technological advances mean that the fabrication of fixed dental prostheses (FDPs) can be simplified through the use of digital impressions and CAD/CAM systems[1]. The major advantages of using digital techniques include more consistent results, including more consistent quality with respect to restoration efforts. Especially when performing full mouth rehabilitation with FDPs, the likelihood of obtaining a satisfactory impression in a single attempt using a conventional impression technique is low. Moreover, it may also be more difficult to transfer a patient's well-adapted occlusal scheme from the provisional phase to definitive prostheses when using conventional techniques rather than a CAD/CAM system. A digital impression, by virtue of its consistency, is an appropriate tool for obtaining an ideal impression. Digital methods also allow for duplication of the morphology of provisional restorations. However, due to the limitations of CAD/CAM systems, prosthesis fabrication cannot depend solely on the use of digital methods. In fact, neither digital nor conventional methods alone can currently meet the requirements of functional and esthetic quality[2]. Rather, the combined use of both analog and digital workflow techniques is required to achieve the best possible results[3].

The case report presented herein demonstrates how to take final impressions using the intraoral scanner method along with a digital reference model. It further details the fabrication of monolithic zirconia fixed prostheses with CAD/CAM technology in posterior areas combined with the application of porcelain layering on anterior teeth.

Case Report

An 80-year-old male patient with a medical history of cerebrovascular disease and Parkinsonism presented with full mouth FDPs. He complained about throbbing pain over his upper right back teeth, and he had his right maxillary molars extracted due to extensive undermining caries and pulpitis. The patient was referred from the general dental practitioner with the objective of restoring his missing teeth. Routine radiographic examinations consisting of periapical and bite-wing films were taken (Fig. 1). Intra-oral examination showed that most of the prostheses presented with overhang combined secondary caries (Fig. 2). Thus, the decision was made to remove all the ill-fitted splinting prostheses and then conduct a further evaluation (Fig. 3). Tooth 21 and tooth 31 were extracted due to compromised structure resulting in poor prognosis (Fig. 4). In discussions with the patient, a final treatment plan consisting of FDPs and implants was advised, and teeth 28, 38, and 48 were extracted because of the difficulty of self-maintenance. Moreover, endodontic treatments were arranged as indicated in Table 1, and periodontal phase I therapies were arranged as indicated in Table 2.

Fig. 1: Dental radiographic images before treatment

Fig. 2: Initial photographs illustrating obvious gingival inflammation

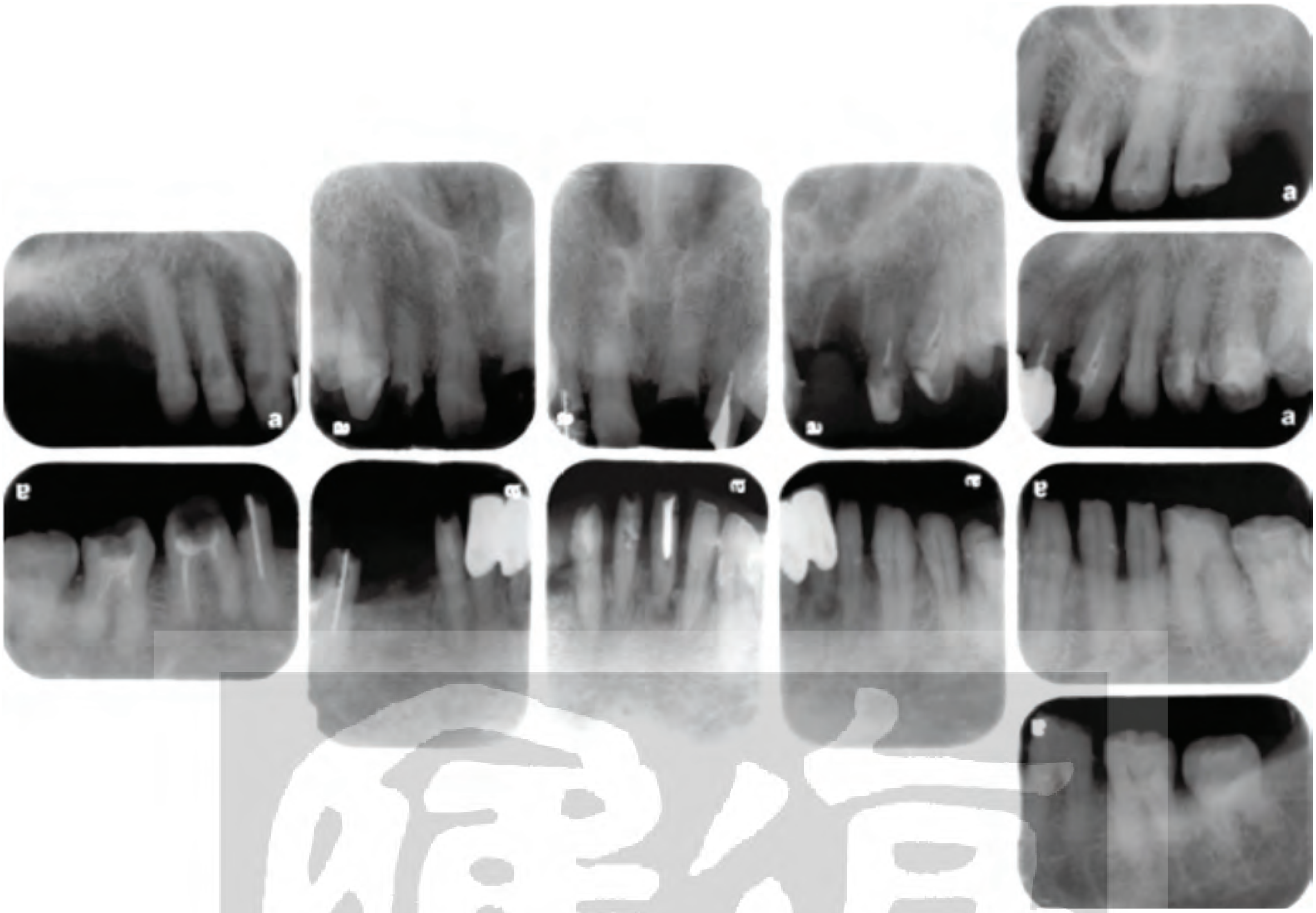

Fig. 3: Dental radiographic images after removal of FDPs.

Fig. 4: Tooth structure evaluation after removal of FDPs and extraction of teeth 21 and 31.

Table 1

Previous endodontic treatment	12, 22, 23, 25, 26, 31, 41, 42, 45, 46, 47
Pulp necrosis	14, 27, 34, 36
Pulpitis	11, 13, 35
Endodontic retreatment	12, 22, 23, 25, 26, 41, 42, 45, 46, 47
Endodontic treatment	11, 13, 14, 27, 34, 35, 36

After the removal of all the ill-fitted FDPs, primary impressions were made using irreversible hydrocolloid impression material (CA38, CAVEX, Holland) and were then poured with dental stone (NEO PRIMESTONE, Mutsumi, Japan) to fabricate the study casts. The study casts were then mounted in centric relation on a semiadjustable articulator (Artex Arcon CPR, Amann Girrbach AG, Austria) using a facebow transfer technique. A diagnostic wax-up was then made in order to fabricate the provisional restorations and to analyze the space of the implant areas (Fig. 5). The occlusal scheme was designed using the group function. The space between the tooth 43 and 44 areas was 2 mm too short for two 4-mm-diameter implants (Fig. 6). The definitive plan was therefore modified from two implant-supported FDPs to a tooth-implant-supported fixed prosthesis.

The PMMA (Alike, GC America) provisional restorations were fabricated with the indirect-direct technique. Cone beam CT images were taken with vacuum form surgical

Table 2

Distal			Buccal			Mesial		
	18	17	16	15	14	13	12	11
A.L.				6 2 4	3 4 6	5 2 5	4 3 3	4 3 6
P.D.				3 2 3	3 4 6	5 2 5	4 2 2	3 3 5
P.D.				2 2 3	3 2 6	4 2 3	4 2 3	3 2 2
A.L.				4 4 3	5 4 6	5 4 5	5 3 3	3 3 3
Mobility				0	0	0	0	0
F.I.				0 0	0 0			
Palatal								

Mesial			Buccal			Distal		
	21	22	23	24	25	26	27	28
A.L.		2 2 3	2 2 3	3 3 3	3 2 2	2 2 2	4 3 3	4 3 3
P.D.		2 2 3	2 2 3	3 3 3	3 2 2	2 2 2	4 3 3	4 3 3
P.D.		3 2 3	4 2 3	3 2 3	3 3 3	3 2 3	3 2 3	3 3 3
A.L.		3 2 3	4 2 3	3 2 3	3 3 3	3 2 3	3 2 3	3 3 3
Mobility		0	0	0	0	0	0	0
F.I.				0 0	0 0	0 0	0 I 0	0 0 0
Palatal								

Mesial			Lingual			Distal		
	31	32	33	34	35	36	37	38
A.L.	2 2 8	3 3 3	3 2 3	3 2 4	4 3 3	3 3 3	3 3 4	4 3 4
P.D.	2 2 8	3 3 3	3 2 3	3 2 4	4 3 3	3 3 3	3 3 4	4 3 4
P.D.	4 2 3	3 2 3	3 2 3	3 2 4	5 4 3	3 3 3	3 4 4	5 6 5
A.L.	4 2 3	3 2 3	3 2 3	3 2 4	5 4 3	3 3 3	3 4 4	5 6 5
Mobility	I	0	0	0	0	0	0	0
F.I.						I I	0 0	I I
Buccal								

Mesial			Lingual			Distal		
	48	47	46	45	44	43	42	41
A.L.	5 3 4	5 4 4	4 4 3	2 2 3			2 2 3	3 2 3
P.D.	5 3 4	5 4 4	4 4 3	2 2 3			2 2 3	3 2 3
P.D.	3 4 3	6 2 4	3 3 3	3 2 3			2 2 4	4 2 3
A.L.	3 4 3	6 2 4	3 3 3	3 2 3			2 2 4	4 2 3
Mobility	I	0	0	0			0	1
F.I.	I I	0 0	I I					
Buccal								

Fig. 5: Full mouth diagnostic wax-up.

stents placed on the provisional restorations to determine the proper site for dental implant placement (Fig. 7). The Astra Tech implant system was selected according to the available bone. An OsseoSpeedTM TX implant (4.0 x 10mm) (Astra Tech, Dentsply Sirona, USA) was inserted over the tooth 43 area combined with the GBR technique by FDBA and resorbable collagen membrane (EZ CureTM, Biomatlante, France). Another implant (5.0 x 10mm) was placed over the tooth 16 area. Both implants were inserted using the surgical stent. The provisional prostheses were delivered after 4 months of osseointegration (Fig. 8). The occlusion evenly contacted in the central fossa in the maximum intercuspal position (MICP), while the anterior teeth and implants 16 and 43 exhibited light contact with the opposing teeth. Furthermore, the occlusal scheme was set using the group function: teeth 13, 14, and 15 were in contact with teeth 43-X- 45 and 46, except that implant 16 was disoccluded when the lateral excursion was processing (Fig. 9).

Fig. 6: Space analysis showing the space was 12mm

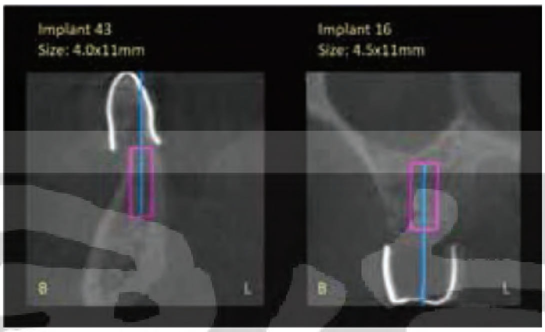

Fig. 7: Implant site and implant size planning in computer software

Fig. 8: Provisional restorations in MICP

Fig. 9: Provisional restorations in lateral excursion

To ensure that no complications occurred, periodic follow-ups were carried out for 6 months. Afterward, the patient was ready for the final impressions.

A digital impression of the provisional restorations was taken using an intraoral scanner (CS 3500, Carestream, USA) and served as a reference (Fig. 10), after which digital final impressions were taken using the double-cord technique and scan-bodies (Fig. 11). A dentition framework was scanned first to minimize the distortion, after which the marginal area of the virtual impression was cut. The second retraction cords were then removed one by one, after which scanning of the exposed marginal area was performed. In order to maintain the vertical dimension and occlusal relationship, the occlusal record on one side was scanned with provisional restorations on the other side. As for the emergence profiles of the implant restorations, the provisional restorations were attached to implant-analogs and scanned extraorally, and then the images were matched with the digital reference models (Fig. 12).

A dental CAD software (exocadTM, Germany) was used to design the restorations. Matching the virtual reference casts with the virtual working casts by using the digital cross mounting technique (Fig. 13) makes the function and the contours of the digital wax-up just the same as those of the provisional restorations[4] (Fig. 14). The anterior FDPs had a zirconia framework with porcelain veneering, and the posterior FDPs were monolithic prostheses (Fig. 15). It should be noted that the guidance area of maxillary incisors should remain untouched

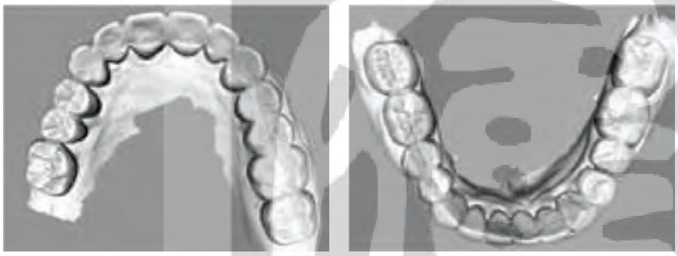

Fig. 10: Digital reference models

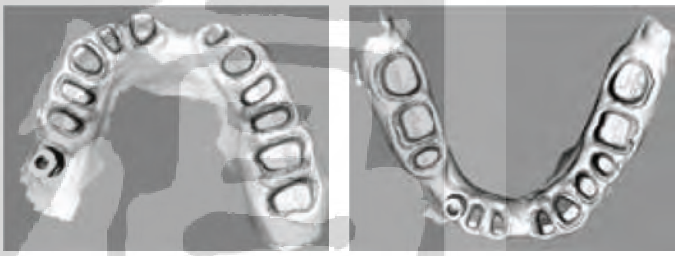

Fig. 11: Digital final impressions

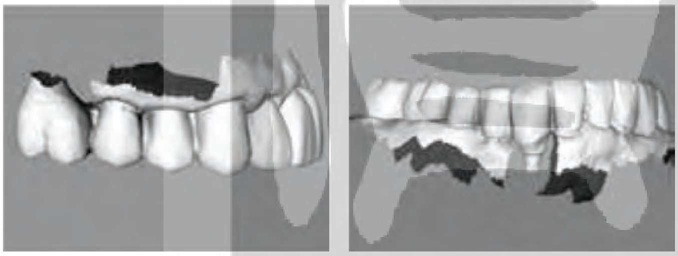

Fig. 12: Duplication of emergence profile

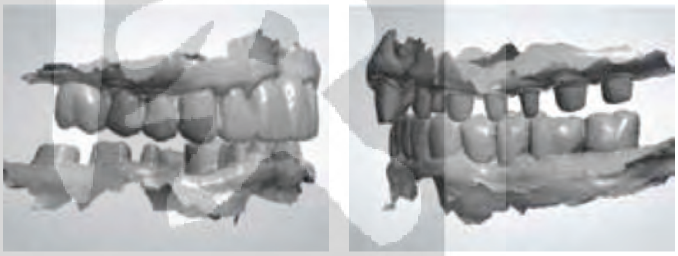

Fig. 13: Digital cross mounting

Fig. 14: CAD file of full mouth digital wax-up

Fig. 15: CAD file after virtual cutback, prior to milling

while performing the virtual cutback to precisely preserve the functional morphology of the provisional restorations. In order to maintain the original anterior guidance, a traditional customized incisal guide table was fabricated by using reference models of the provisional restorations.

In order to obtain retrievability and rigid fixation of the tooth-implant-supported FDP simultaneously, a customized abutment of implant 43 and a coping of tooth 45 were fabricated (Fig. 16). All the prostheses were fabricated in zirconia using CAD/CAM technology.

The posterior monolithic crowns, frameworks, coping, and customized abutments were tried in. Once all the restorations were adjusted and the occlusion was stable, a conventional pick-up impression was performed by using a stock tray with polyvinyl siloxane impression material (Aquasil Ultra, DENTSPLY Caulk, USA) (Fig. 17). In addition, facebow records were taken to assist in determining the incisal plane. Porcelain was then fired onto the zirconia frameworks of the anterior teeth.

Finally, all the restorations were tried in again and delivered. The customized implant abutments of 43 and 16 were torqued to 20N and 25N, respectively, as recommended by the manufacturer. A second torque was applied ten minutes after the initial tightening torque. The coping of tooth 45 was cemented using self-adhesive resin cement, and the final implant restorations were cemented with polycarboxylate cement. The rest of the FDPs were cemented using self-adhesive resin cement (RelyXTM Unicem, 3M ESPE, Seefeld, Germany), and all the restorations exhibited accurate marginal fitness, as well as stable occlusion with satisfactory esthetic outcomes (Figs. 18-19).

Discussion

At present, digital technology plays a major role in our daily lives, both in society in general and in dentistry in particular. In the latter area, digital protocols are gradually influencing prosthodontic treatment concepts[5].

The CAD/CAM production of monolithic prostheses, originated from intraoral scanning

Fig. 16: Photograph showing a customized abutment of implant 43 and a coping of tooth 45.

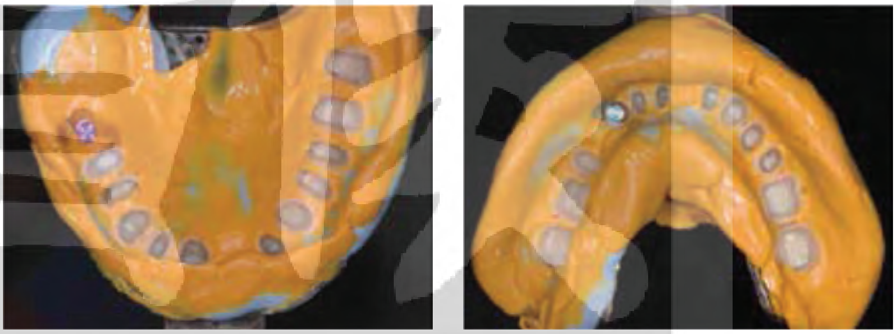

Fig. 17: Pick-up impression.

Fig. 18: Definitive zirconia prostheses, after insertion.

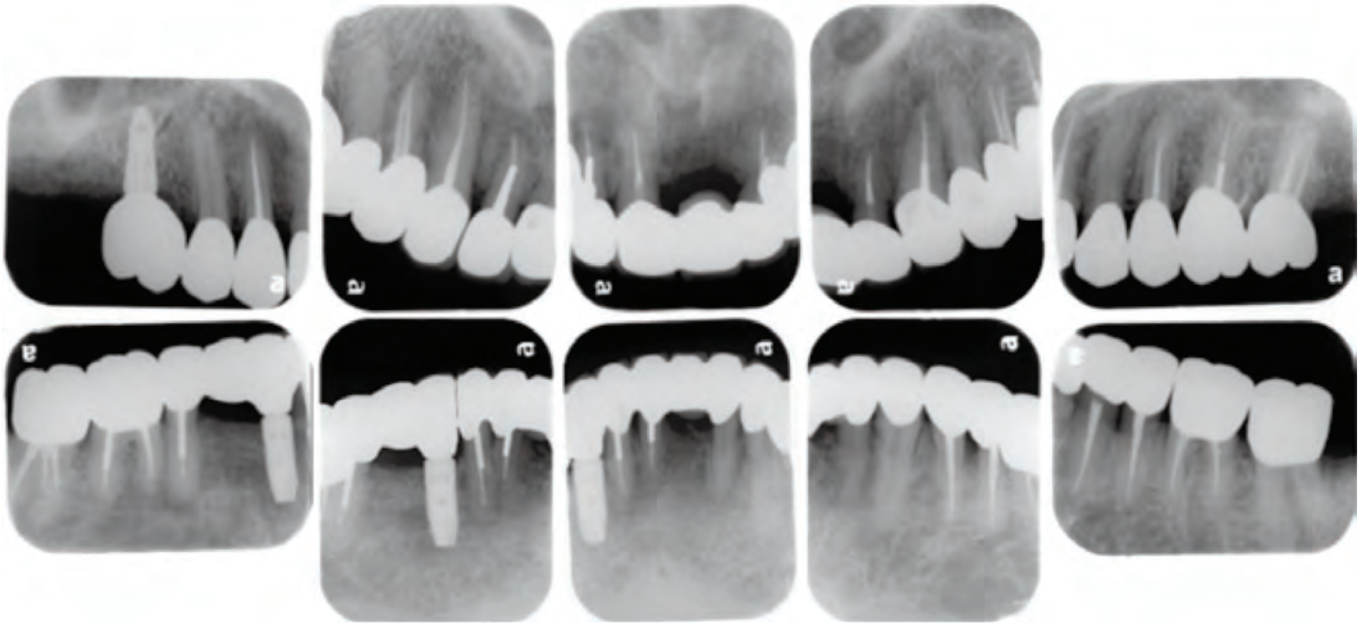

Fig. 19: Dental radiographic images after treatment

followed by a virtual design and production, might benefit from the use of the digital workflow[1]. By using digital procedures, clinicians can avoid the need for physical models and the space needed to store them. Moreover, the delicate abutment margins on the working cast will not be chipped off during laboratory processing. Also, the digital data can be saved, such that the exact same prosthesis can be fabricated immediately if a remake is needed.

However, with the inherent limitations of zirconia, it is difficult to achieve a natural appearance in the esthetic zones. Besides, the chipping rate of porcelain in porcelain-fused-to-zirconia (PFZ) prostheses is higher than that of porcelain-fused-to-metal (PFM) ones[6]. To overcome these problems, mild cutbacks for porcelain veneering in nonfunctional areas can be performed to achieve more esthetic and durable outcomes[7]. Consequently, combining analog with digital work steps might offer the best results[1].

An experienced technician is needed to participate in the actual handcrafting process. Therefore, it is necessary to have a physical working cast made either by a conventional impression method or 3D printing technology. A conventional impression procedure is simple to perform when the number of abutments is small. However, the greater the number of abutments, the more difficult such a procedure will be. In complex cases, utilizing 3D printing technology to fabricate the working casts seems to be an ideal option, but the cost of this approach is higher than that of using conventional impression methods. An alternative method entails taking a pick-up impression when the frameworks are tried. Then the porcelain layer can be applied on the framework.

In order to duplicate the emergence profile of an implant provisional restoration, the gingival contours from the provisional prosthesis need to be transferred. Nowadays, an intraoral scanning device can be used to scan the soft tissue. However, the surrounding peri-implant tissues collapse soon when the provisional prosthesis is removed, which means that only a part of the established emergence profile can be accurately captured. Therefore, it is important to perform such scanning without delay[8].

In this case, provisional restorations were attached to analogs and scanned extra-orally from top to bottom. The images were then matched with the digital reference models. With CAD/CAM technology and the correct methodology, the established emergence profile of an implant provisional restoration can be duplicated in the final restoration in an accurate way.

Because of the inherent differences between teeth and implants, especially in their supporting mechanisms and survival rate, the subject of connecting implants to teeth has been a controversial in the last several decades[9]. Complications associated with tooth-implant-connected prostheses have been categorized into biological and technical types. Previous short-term clinical studies have reported that the tooth-implant-supported prostheses did not have a higher risk of technical or biological failure than implant-supported ones for up to 5 years of clinical usage[10]. On the other hand, tooth-implant-supported prostheses have been reported by one study to have a higher failure rate than implant-supported prostheses after 10 years of follow-up[11]. However, no statistical analysis has substantiated that finding.

The implant-supported fixed prosthesis seemed to be the ideal option in this case. However, the space between the tooth 43 and 44 areas was 2 mm too short for two regular 4-mm-diameter implants. So, the treatment plan was modified from two implant-supported prostheses to a tooth-implant-supported fixed prosthesis. In such a scenario, nonrigid attachments and temporary cements should be avoided as they will increase the incidence of tooth intrusion. Therefore, polycarboxylate cement (DurelonTM polycarboxylate cement, 3M ESPE, Seefeld, Germany) was used to cement the tooth and implant to avoid the intrusion complication[12]. Furthermore, lateral forces and unbalanced tooth contacts should be minimized in centric and excursive movement, and frequent occlusal adjustment is an important follow-up step[9]. Consequently, implant 16 was disoccluded during lateral excursion, and the occlusal scheme was set using the group function in order to make sure that premature occlusal contacts were avoided.

An alternative treatment plan for restoring a mandibular second premolar consists of making a mesial cantilever FDP reaching from the mandibular first molar. According to Pjetursson BE et al., the 5-year and 10-year survival rates of cantilever FDPs are similar to those of tooth-implant-supported FDPs[10]. However, a single cantilevered pontic requires at least two abutments[14]. This means that the first and second molar must be splinted for a second premolar cantilevered pontic. In this circumstance, those splinted molars become an area for which hygiene would be difficult to maintain for an elderly individual with Parkinsonism.

Taking a conventional impression of multiple abutments is a difficult task. The approved "occlusion" of provisional restorations should be transferred by a cross-mounting technique, which is time consuming. Moreover, even such a technique cannot transfer the whole "contour". With the help of CAD/CAM technology, however, the prosthetic contours of provisional restorations can easily be duplicated to the definitive prostheses[13].

Reference

1. Tim Joda, Fernando Zarone, Marco Ferrari. The complete digital workflow in fixed prosthodontics: a systematic review. BMC Oral Health. 2017; 17: 124.
2. Weston J. Closing the gap between esthetics and digital dentistry. Comp Cont Educ Dent. 2016;37(2):84–91.
3. Patel N. Integrating three-dimensional digital technologies for comprehensive implant dentistry. J Am Dent Assoc. 2010;141(Suppl 2):20S–24S.
4. Fasbinder DJ. Digital dentistry: innovation for restorative treatment. Comp Cont Educ Dent. 2010;31(4):2–11.
5. Linkevicius T, Vaitelis J. The effect of zirconia or titanium as abutment material on peri-implant soft tissues: a systematic review and meta-analysis. Clin Oral Implants Res. 2015;26(suppl 11):139–47.
6. Cheng CW, Chien CH, Chen CJ, Papaspyridakos P. Complete-mouth implant rehabilitation with modified monolithic zirconia implant-supported fixed dental prostheses and an immediate-loading protocol: a clinical report. J Prosthet Dent. 2013;109:347–52.
7. Ioannis Papadopoulos, Georgia Pozidi, Hercules Goussias, Stefanos Kourtis. Transferring the emergence profile from the provisional to the final restoration. J Esthet Restor Dent. 2014;26(3):154-61.
8. Safoura Ghodsi, Sasan Rasaeipour. Tooth-implant connection: A literature review. World J Dent, 2012;3(2): 213-9.
9. Vidya Kamalaksh Shenoy, Shobha J Rodrigue, E Prashanti, Sharon J. R. Saldanha. Tooth implant supported prosthesis: A literature review. J Interdiscip Dentistry. 2013; 3(3): 143-50.
10. Lindh T, Dahlgren S, Gunnarsson K, Josefsson T, Nilson H, Wilhelmsson P, Gunne J. Tooth-implant supported fixed prostheses: A retrospective multicenter study. Int J Prosthodont. 2001;14(4):321-8.
11. L. Arcuri, C. Lorenzi, F. Cecchetti, F. Germano, M. Spuntarelli, and A. Barlattani. Full digital workflow for implantprosthetic rehabilitations: a case report. Oral Implantol. 2015 Oct-Dec; 8(4): 114–21.

Original Article

Optimizing the Insertion Positions And Angles of Implants for All-on-Four Dental Prostheses

Running title: Shape optimization of all-on-four prosthesis

Yung-Chung Chen
Department of Stomatology, Division of Prosthodontics, National Cheng Kung University Hospital, College of Medicine, National Cheng Kung University, Tainan, Taiwan
Institute of Oral Medicine, College of Medicine, National Cheng Kung University, Tainan, Taiwan

Chi-Lun Lin
Department of Mechanical Engineering, National Cheng Kung University, Tainan, Taiwan

Yu-Feng Huang
Department of Mechanical Engineering, National Cheng Kung University, Tainan, Taiwan

Corresponding authors:

Yung-Chung Chen, DDS., M.Dsc, PhD
Assistant Professor, Institute of Oral Medicine, College of Medicine, National Cheng Kung University, Tainan, Taiwan
Email: yc_chen@mail.ncku.edu.tw
Phone: +886-6-2353535 ext. 6713

Chi-Lun Lin, MS., PhD
Assistant Professor, Department of Mechanical Engineering, National Cheng Kung University, Tainan, Taiwan
Email: linc@mail.ncku.edu.tw
Phone: +886-6-2757575 ext. 62190

DOI: 10.6926/JPI.201812_7(4).0004

Abstract

Objectives: The all-on-four concept is an alternative option of full-arch rehabilitation for fully edentulous patients. However, its structural design and mechanical performance have not been comprehensively investigated. This study was aimed to optimize the placement of dental implants and prosthetic configuration used in all-on-four treatment by a numerical approach in which the finite element analysis (FEA) and design optimization techniques were integrated to minimize the peri-implant strain for reducing the risk of early bone loss.

Methods: In the numerical model, the fixed prosthesis is supported by four implants including two posterior tilt implants and two anterior axial implants over mandible bone, and subject to a distributed force of totally 150N in the occlusal direction. The design variables are the length, diameter, position and two tilt angles of the distal implants. An automated framework was implemented to generate various simulations with given design configurations. The Nelder-Mead method was introduced to iteratively search for the optimal design that minimizes the minimum principal strain in the distal peri-implant region.

Results: Given a clinically used design with [distal implant tilt angle, distal implant length, distal implant diameter] = [30°, 11.5 mm, 4.0mm] as the start point, the search process converged after 200 iterations, which took 52.45 hours of computation time. The total volume of elements in distal peri-implant bone with a minimum principal strain below -0.004 was improved 40.15%, from 7.25 mm^3 to 4.35 mm^3. By adjusting the penalty factor of the optimization algorithm, the computation time was significantly reduced to 16.20 hours.

Conclusion: This research developed an automated framework for optimizing the implants placement based on the FEA and iterative searching algorithm. The results showed that the structural design of prosthesis was improved through the optimization process. The automated framework can be further developed for clinical uses to provide treatment suggestions.

Key words: All-on-four dental prosthesis, automated modeling, finite element analysis, shape optimization

Introduction

Nowadays, implants-supported prosthesis is an alternative treatment option for completely edentulous patients who do not favor wearing removable dentures. Six implants or more are usually used for full-arch rehabilitation. However, it was found in most of edentulous jaws that the resorption in the distal region and poor bone quality are observed[1, 2]. Sufficient and adequate bone quantity is the first requirement to ensure long-term survival of dental implants. To achieve that, bone grafting in mandible and sinus augmentation in maxilla should be conducted in these cases, which would cause a longer procedure time and a higher risk of complication.

The all-on-four treatment concept, which only uses four implants to support prostheses, is a new option for edentulous patients[3, 4]. The surgical principle of the all-on-four treatment concept is to place two axial implants in the anterior region and two tilted implants at the distal end. The tilted distal implants are able to prevent from traumatizing some anatomical structures, for example, the mental foramen in the mandible and maxillary sinus in the maxilla. In addition, some more advanced and complex procedures can also be avoided such as sinus lifting with bone grafting[5]. According to clinical research, cumulative survival rate of all-on-four treatment at follow-up of 12, 24, 36 months is 98.6%, 99.1%, and 99.0% respectively[6]. It can be a cost-effective and time-efficient treatment option for fully edentulous patients.

Although changes in the bone level surrounding the implants of all-on-four treatment were found acceptable in the first few years' follow-up[6-8], many factors can still influence its long-term survival such as peri-implantitis and mechanical failure of prosthesis. More cautious care is required for the surrounding implants tissue health, especially for the tilted implants. Because of using fewer number of implants, it is extremely important to secure each implant's survival. Loss of any implant can reduce the lifetime of the supported prosthesis. In addition, the mechanical factors including occlusal scheme, material selection and stress distribution must be evaluated more carefully. When overloading occurs, resorption of the alveolar bone can be worsen especially in peri-implant region, which further increase the risk of prosthetic failures[9, 10]. For the above reasons, a comprehensively mechanical analysis is necessary to be conducted.

The Finite Elements Method (FEM) is efficient for studying the mechanical structure and has also been widely used in the industry of dental implants. By using FEM, researchers compared mechanical behavior between all-on-four and other fixed prostheses treatments. The results showed that using six or more implants as the fixed prostheses produced smaller peri-implants stress than the all-on-four treatments, however, the maximum stress of all-on-four did not exceed the load resistance of bone[2, 11]. Although the mechanical performance is poorer than other fixed prostheses, the advantages of shorter processing time and lower computing cost make the all-on-four concept an alternative option clinically. It is believed that reducing the peri-implant stress of the structure could make all-on-four prosthesis more reliable. Recent study showed that the configuration and geometry of implants play an important part in the peri-implant stress of all-on-four treatment. By changing tilt angle, length, diameter and cantilever length of implants, it is possible to reduce the stress and strain in peri-implant area[9].

Some researchers proposed that shorter cantilever length results in lower peri-implant stress[12]. Some studies manipulated the tilt angle to obtain different cantilever lengths. The results showed that the model with the tilt angle of 45°, which resulted in the shortest cantilever length, produced the lowest peri-implant stress[13]. In other studies of the all-on-four numerical model, higher peri-implant stress was found around the tilt implants than the axial implants when the positions of the implants were fixed[14, 15]. In other words, increasing tilt angle without varying cantilever length can cause higher peri-implant stress.

According to the researches about all-on-four's parameter, the cantilever length is determined by not only tilt angle but also position of implants[13, 16]. In addition, the length and diameter of implants can affect the mechanical behavior. The study using a multi-parametrical model showed that the matching relation between the parameters should be concerned in order to find the best design for all-on-four treatment[17].

In the present study, a comprehensive mechanical analysis for the all-on-four treatment was conducted to investigate the optimal position and orientation for placing the dental implants.

In addition, an automated modeling framework was proposed to become a part of the treatment evaluation process. The automated modeling enables an automatic process that incorporates the design optimization searching algorithm and finite element analysis to iteratively optimize the alignment of the implants.

MATERIALS AND METHODS

The 3D geometry of an edentulous mandible was imported to construct a finite element model in ABAQUS 6.14 (Simulia by Dassault Systemes, France), and feature points were defined to form the supporting framework of prosthesis. As a result, the framework can be determined by a parabolic curve which fits these given feature points. The implants were positioned along the curve, as shown in Figure 1. The design of the implants was referred from the manufacturer, as shown in Figure 2. To simplify the FEA model, the thread of the implants is neglected. The model was meshed by using tetrahedral elements, and the element size was set as 0.8 mm according to our convergence analysis, which resulted in about 320,000 nodes and 1,600,000 elements. The material properties are shown in Table 1, and the materials are assumed to be homogeneous and isotropic. The materials of the implants and framework used were titanium (Ti). An axial load of 150 N was applied to both sides of the distal end of the framework which can form a larger moment arm.

The model for design optimization includes eight design variables (Figure 3), which are the both sides of the distal implants' tilt angles, lengths, diameters, and positions, and the symbols are chosen as ϕ_{right}, L_{right}, d_{right}, θ_{right}, ϕ_{left}, L_{left}, d_{left} and θ_{left} respectively. The design space is defined by the following constraints:

$0° \le \phi_{right} \le 45°$

$8 \le L_{right} \le 12 (mm)$

$3 \le d_{right} \le 5 (mm)$

$35° \le \theta_{right} \le 45°$

$0° \le \phi_{left} \le 45°$

$8 \le L_{left} \le 12 (mm)$

$3 \le d_{left} \le 5 (mm)$

$40° \le \theta_{left} \le 50°$

The objective was to minimize the total volume of elements with a minimum principal strain below -0.004[18, 19]. Additional four constraints, interference and mandibular nerve, are derived to avoid the implant constructed by automated algorithm interferes the mandibular nerve. Two interference constraints were then applied to the both sides of the distal implants. An illustration of the constraints is shown in Figure 4, and the equation is shown below, where $t_{tolerance}$ is the distance between distal bound and anterior bound.

$$t - L\sin(\phi) + \frac{d}{2}\cos(\phi) < t_{tolerance}$$

Two mandibular nerve constraints shown in Figure 5 are applied to both sides of the distal implants. The equation of the constraints is shown below, where h_{nerve} is the depth of the mandibular nerve which is set to 6mm for on both sides, and t is the distance between the implant and mandibular nerve

$$\frac{\frac{d}{2}\cos\phi - t}{\tan\phi} < h_{nerve}$$

To search for the optimal solution, the numerical optimization method, the Nelder-Mead method was applied. The exterior penalty method was used to treat the constrained optimization problem of this study. The method introduced a penalty factor to add a penalty value to the objective function of those design points outside the feasible region. A large penalty factor would magnify the penalty more to eliminate infeasible designs. Several penalty factor values were tested, and the values of 100 and 200 were compared and discussed. The flow chart of the automated modeling and mechanical analysis is shown in Figure 6.

To validate the finite element model, an in vitro experiment was conducted to compare the measured and simulated strain values. By using the automated framework developed by present study, another optimization was conducted by using the same material as the experimental model. For the experiment, four implants were placed into two 3D printed mandibular models with the initial prosthesis design and the optimal prosthesis design (Figure 7). For both cases, an axial load of 150 N was applied to the distal end of the prosthesis (Figure 8) and the strain value was measured at 5mm away from the center of the distal implants in the distal direction. The strain value was compared with that probed at the same location of the finite element model.

RESULTS

The optimization process was started with an initial design of 4 mm in diameter, 11.5 mm in length and tilt angle of 30° for the posterior implants and 3.4 mm in diameter, 8.5 mm in length and tilt angle of 0° for the anterior implants, a design currently used in clinical practice. In the first run, the penalty value was set for 100. After 150 iterations of the Nelder-Mead method, the condition of convergence was met. The optimal design point was found in an infeasible region, close to the boundary of the left mandibular nerve constraint. A second run of the Nelder-Mead method was then performed with penalty value of 200. After 150 iterations, the convergent condition was met. The optimal designs obtained by two separate runs of the optimization process are shown in Table 2.

The volume with a minimum principal strain below -0.004 in peri-implant region is shown in Figure 9. The objective value of the optimal design decreased by 40.15% compared to the initial one. The plot of minimum principle strain for the initial design and optimal design was shown in Figure 10. The high strain region, which is close to the lingual side, became smaller after the optimization. In addition, there does not exist elements whose minimum principal strain is below -0.004 in all the anterior peri-implant regions.

In the finite elements model, there might be singular value on the interface between implants and bone, in addition the maximum value of strain or stress in the region is divergence due to the numerical method. To avoid the defect, the total volume summed by the elements with a minimum principal strain below -0.004 is regarded as the indicator of the mechanical structure. And the results showed that using this objective function successfully improved the mechanical performance of the structure.

DISCUSSION

It was observed that the design point searched in each iteration tended to move toward both sides of the mandibular nerve constraints. Therefore, a parametric study was further conducted to investigate the local region around the optimal design point obtained by using the automated framework. The result is shown in Figure 12, Figure 13, Figure 15 and Figure 16.

In our study, the design variables which can directly change the cantilever length are θ_{right} and θ_{left}. By reducing these two variables, the positions of the implants were moved toward the distal end, and the cantilever length was shortened. Since moving the distal implants toward the distal end is restricted by the mandibular nerve constraints (Figure 11 and Figure 14), the distal implants must be placed near the edge of the foramen. However, along with the mandibular nerve constraints, increasing θ resulted in the increase of tilt angle ϕ (Figure 12 and Figure 15). Thus, to avoid the high stress caused by excessive tilt angles, the tilt angle must be considered when reducing the cantilever length.

The result of the experiment is shown in Figure 17 and Figure 18. The error between experiment and simulation resulted from the gap between the implant neck and mandibular in experimental model. Observing the objective values of the optimal and initial designs, the difference of strain between left and right implants in the experiment is similar to the difference found in simulation. As a result, we can consider that the FEM model is able to simulate the mechanical behavior corresponding to design changes.

This study certainly has limitations. First of all, the thread of the implants can be added to simulate more realistic results. However, for the optimization purpose of this study, the thread would not significantly affect mechanical behavior of the bone in the peri-implant area. Secondly, the maximum stress and strain values observed in the FEA results could not be used to compare the performance of designs. The singularities occurred in the computation due to many contacts between geometric parts and at sharp edges of the irregular geometry. This explains partially the reason why we used the total volume of elements with a strain value lower than threshold as the objective function rather than the maximum strain. Finally, the automated modeling framework occasionally stopped in the middle of the process due to an error of auto-meshing, which requires a manual intervention to continue a stopped run. Future improvement can replace the built-in mesh function with a more powerful feature.

CONCLUSION

This research developed an automated framework for optimizing the placement of implants of the all-on-four treatment based on the FEM and optimization searching algorithm. By reducing the volume with a minimum principal strain below -0.004 in peri-implant region, the mechanical performance of the prosthetic structure was improved. With the advance of the computing power, the automated framework can produce optimal designs in a timely manner such that biomechanical analysis of dental implant treatment can be delivered in the surgical planning stage.

To conclude, three findings from the present study should be mentioned. Firstly, the positions and tilt angles of the distal implants on the both sides play an important part in the mechanical performance of the all-on-four treatment. Secondly, when selecting designs along the mandibular nerve constraint, the increase of the strain value in the bone caused by tilting the implant was more significant than the decrease of that caused by shortening the cantilever length. Finally, the implants should be placed close to the mandibular nerve to obtain minimal peri-implant strains, which might not be favored by clinicians. Therefore, further investigation is a must.

Table 1

The material properties of the components used in the FEA model[12]

	Young's modulus (MPa)	Poisson ratio
Cancellous bone	1370	0.3
Cortical bone	13700	0.3
Ti	110000	0.3

Table 2

The configurations of initial and optimal designs with different penalty factor values applied.

	ϕ_{left} (°)	L_{left} (mm)	d_{left} (mm)	θ_{left} (°)	ϕ_{right} (°)	L_{right} (mm)	d_{right} (mm)	θ_{right} (°)
Initial design	30.00	11.50	4.00	140.00	30.00	11.50	4.00	40.00
Penalty factor:100	22.95	11.41	4.87	141.58	21.43	11.71	4.02	38.47
Penalty factor:200	23.15	11.34	4.89	141.47	21.09	11.61	3.99	38.09

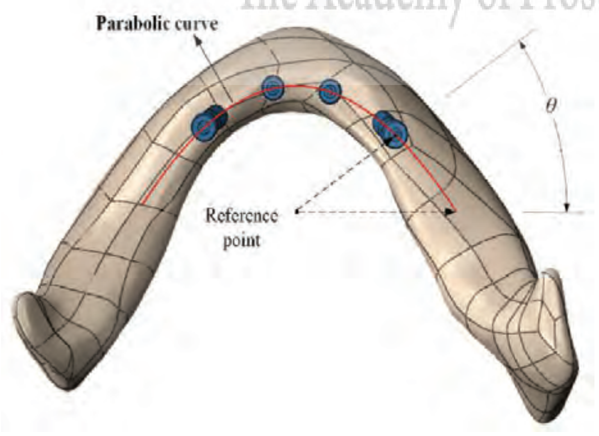

Fig. 1: The positions of implants are defined using a parabolic curve with a reference center point.

Fig. 2: The implant's design contains three parameters: length (L), diameters (d) and tilt angle (Φ).

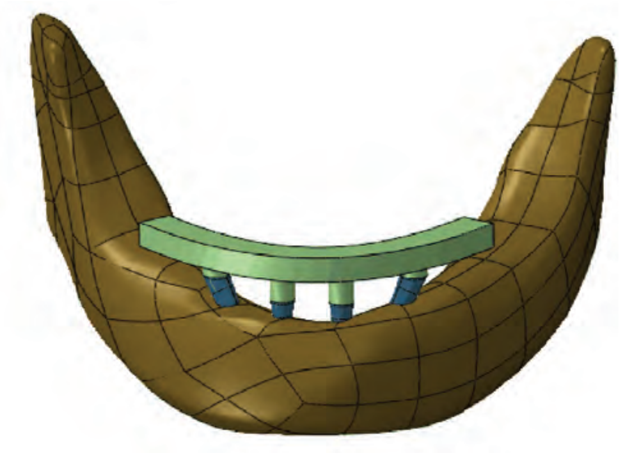

Fig. 3: The geometric model is imported to FEM software.

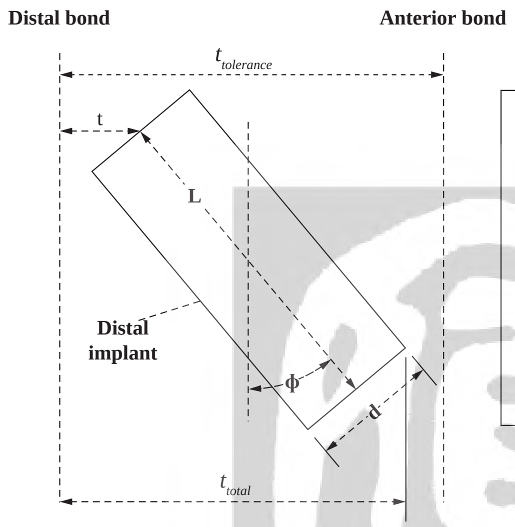

Fig. 4: An illustration of the two interference constraints applied to the both sides of the distal implants, where L is the length, d is the diameter and ϕ is the tilt angle of the implant. Note that the taper and other geometric features are not shown to simplify the illustration.

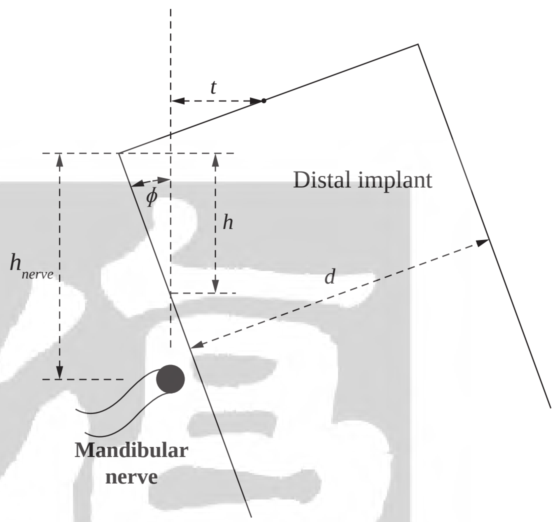

Fig. 5: The relationship between a distal implant and mandibular.

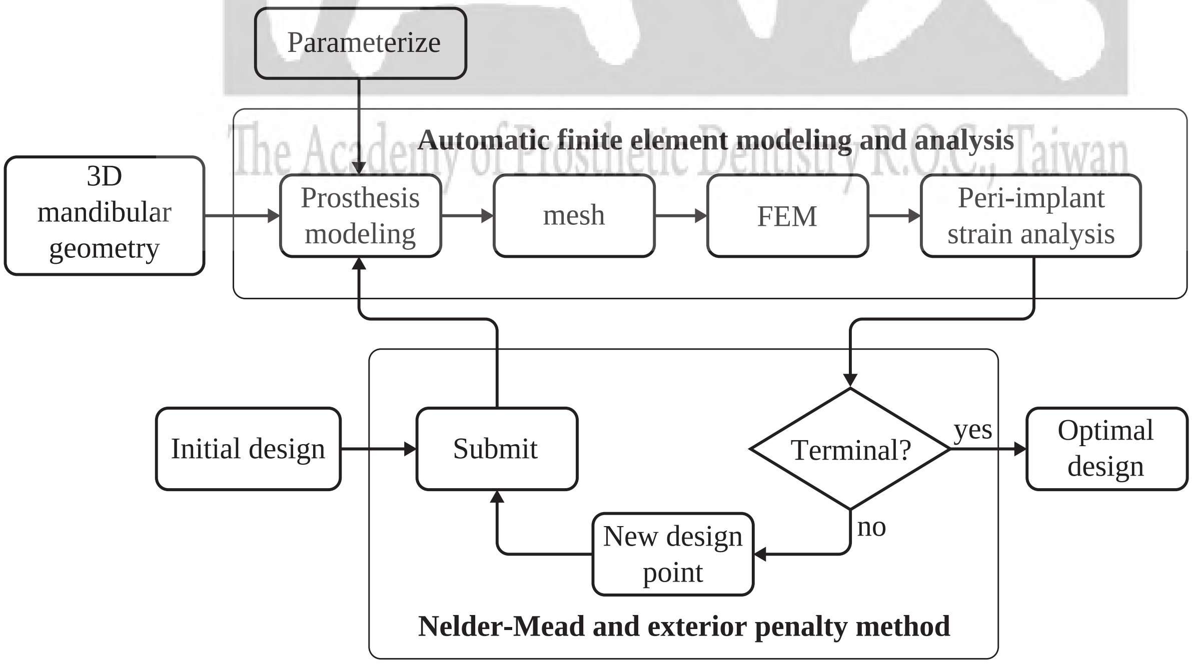

Fig. 6: The flow chart of design optimization combined with automatic modeling for FEA.

Fig. 7: The mandibular model for validation experiment.

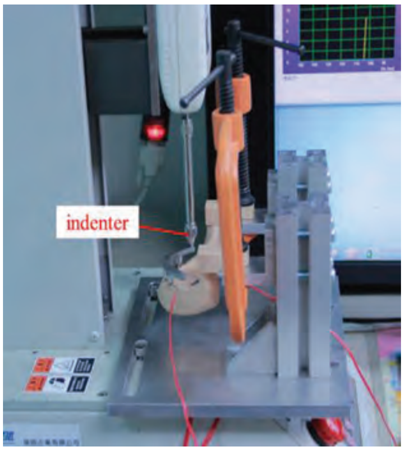

Fig. 8: The experimental setup for loading test, where a mandibular model is fixed by two vises on the frame.

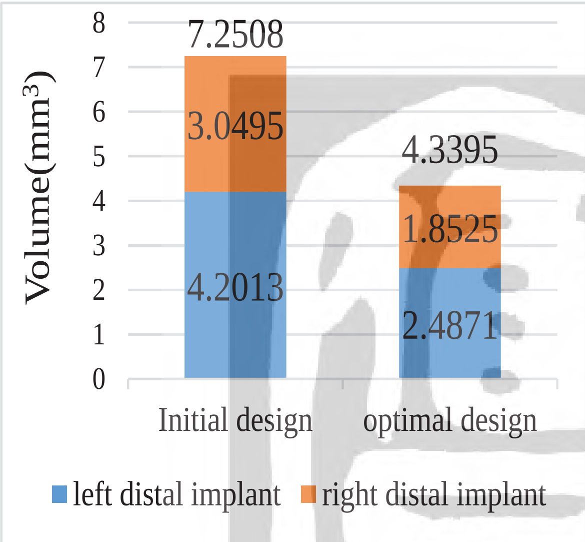

Fig. 9: The total volume of the elements with a minimum principal strain below -0.004 in peri-implant region of distal implants on both sides. The sum of the total volume on both sides is 7.2508 for the initial design and 4.3395 for the optimal design.

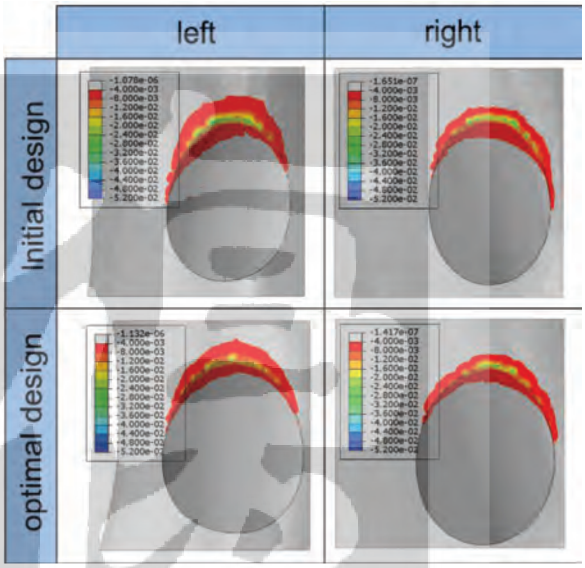

Fig. 10: The top view of the strain contour on the implants. The region with a minimum principal strain below -0.004 is shown in colors.

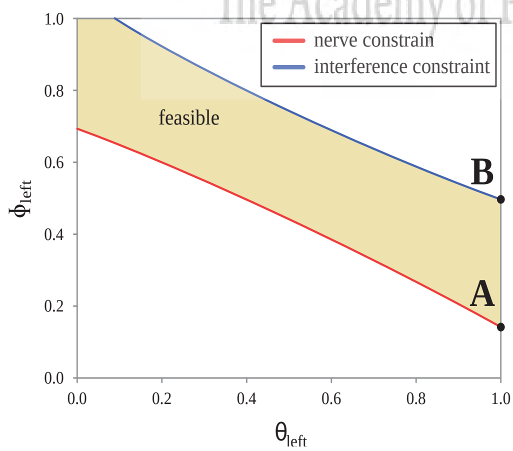

Fig. 11: The feasible region calculated when d_{left} is 5mm.

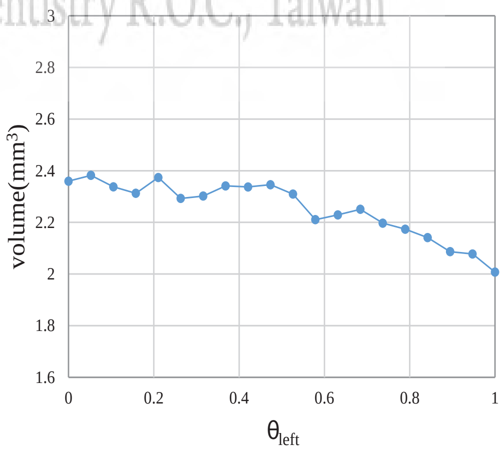

Fig. 12: The value of the objective function versus θ_{left} along the left mandibular nerve constraint.

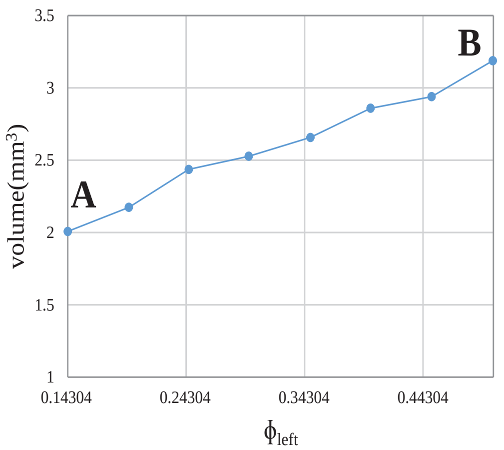

Fig. 13: The value of the objective function evaluated in the range from point A to point B (defined in Figure 11). The minimum is found at point A.

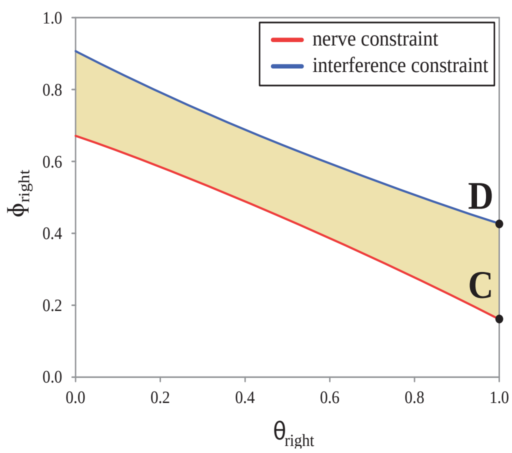

Fig. 14: The feasible region calculated when d_{right} is 5mm.

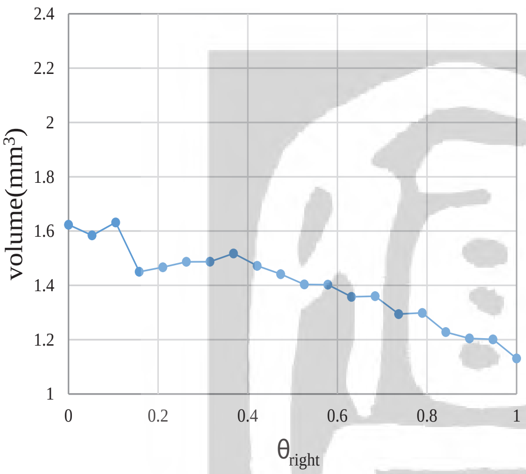

Fig. 15: The value of the objective function versus θright along the right mandibular nerve constraint.

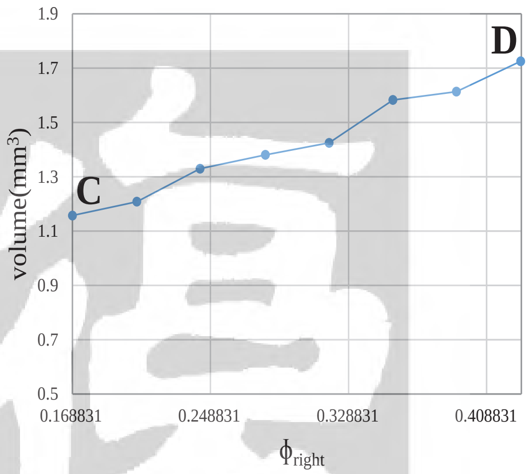

Fig. 16: The value of the objective function evaluated in the range from point C to point D (defined in Figure 14). The minimum is found at point C.

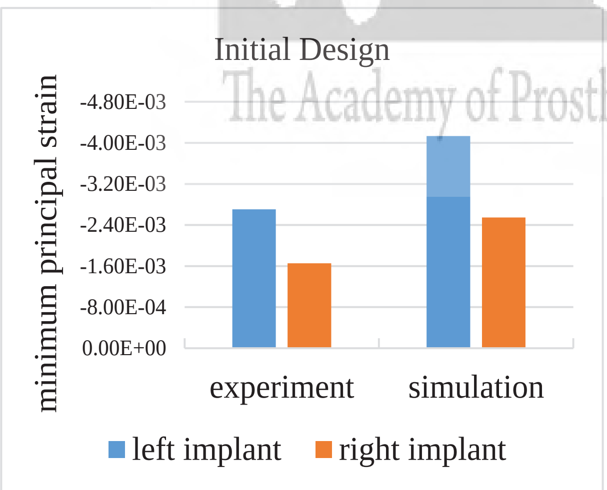

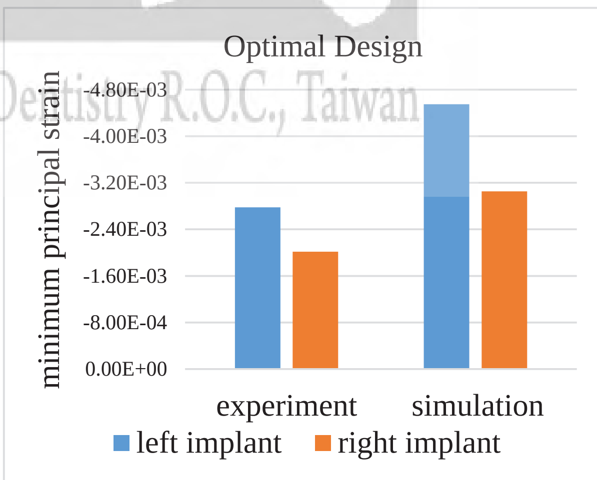

Fig. 17: The minimum principal strain in peri-implant region obtained from simulation and experiment for the initial design.

Fig. 18: The minimum principal strain in peri-implant region obtained from simulation and experiment for the optimal design.

References

1. Gümrükçü Z, Korkmaz YT, Korkmaz FM: Biomechanical evaluation of implant-supported prosthesis with various tilting implant angles and bone types in atrophic maxilla: A finite element study. Computers in Biology and Medicine 2017, 86:47-54.
2. Silva GC, Mendonca JA, Lopes LR, Landre J: Stress Patterns on Implants in Prostheses Supported by Four or Six Implants: A Three-Dimensional Finite Element Analysis. Int J Oral Maxillofac Implants 2010, 25(2):239-246.
3. Malo P, Nobre MD, Petersson U, Wigren S: A pilot study of complete edentulous rehabilitation with immediate function using a new implant design: Case series. Clinical Implant Dentistry and Related Research 2006, 8(4):223-232.
4. Maló P, Rangert B, Nobre M: "All-on-Four" Immediate-Function Concept with Brånemark System® Implants for Completely Edentulous Mandibles: A Retrospective Clinical Study. Clinical Implant Dentistry and Related Research 2003, 5:2-9.
5. Krekmanov L, Kahn M, Rangert B, Lindstrom H: Tilting of posterior mandibular and maxillary implants for improved prosthesis support. Int J Oral Maxillofac Implants 2000, 15(3):405-414.
6. Patzelt SBM, Bahat O, Reynolds MA, Strub JR: The All-on-Four Treatment Concept: A Systematic Review. Clinical Implant Dentistry and Related Research 2014, 16(6):836-855.
7. Adell R, Lekholm U, Rockler B, Brånemark PI: A 15-year study of osseointegrated implants in the treatment of the edentulous jaw. International Journal of Oral Surgery 1981, 10(6):387-416.
8. Del Fabbro M, Bellini CM, Romeo D, Francetti L: Tilted Implants for the Rehabilitation of Edentulous Jaws: A Systematic Review. Clinical Implant Dentistry and Related Research 2012, 14(4):612-621.
9. Geng J-P, Tan KBC, Liu G-R: Application of finite element analysis in implant dentistry: A review of the literature. The Journal of Prosthetic Dentistry 2001, 85(6):585-598.
10. Elsyad MA, Setta FA, Khirallah AS: Strains around distally inclined implants retaining mandibular overdentures with Locator attachments: an in vitro study. J Adv Prosthodont 2016, 8(2):116-124.
11. Fazi G, Tellini S, Vangi D, Branchi R: Three-Dimensional Finite Element Analysis of Different Implant Configurations for a Mandibular Fixed Prosthesis. Int J Oral Maxillofac Implants 2011, 26(4):752-759.
12. Bhering CLB, Mesquita MF, Kemmoku DT, Noritomi PY, Consani RLX, Ricardo Barao VA: Comparison between all-on-four and all-on-six treatment concepts and framework material on stress distribution in atrophic maxilla: A prototyping guided 3D-FEA study. Mater Sci Eng C-Mater Biol Appl 2016, 69:715-725.
13. Bevilacqua M, Tealdo T, Menini M, Pera F, Mossolov A, Drago C, Pera P: The influence of cantilever length and implant inclination on stress distribution in maxillary implant-supported fixed dentures. The Journal of Prosthetic Dentistry 2011, 105(1):5-13.
14. Naini RB, Nokar S, Borghei H, Alikhasi M: Tilted or Parallel Implant Placement in the Completely Edentulous Mandible? A Three-Dimensional Finite Element Analysis. Int J Oral Maxillofac Implants 2011, 26(4):776-781.
15. Kim KS, Kim YL, Bae JM, Cho HW: Biomechanical Comparison of Axial and Tilted Implants for Mandibular Full-Arch Fixed Prostheses. Int J Oral Maxillofac Implants 2011, 26(5):976-984.
16. Baggi L, Pastore S, Di Girolamo M, Vairo G: Implant-bone load transfer mechanisms in complete-arch prostheses supported by four implants: A three-dimensional finite element approach. The Journal of Prosthetic Dentistry 2013, 109(1):9-21.
17. Li XM, Cao ZZ, Qiu XQ, Tang Z, Gong LL, Wang DL: Does matching relation exist between the length and the tilting angle of terminal implants in the all-on-four protocol? stress distributions by 3D finite element analysis. J Adv Prosthodont 2015, 7(3):240-248.
18. Frost HM: Skeletal structural adaptations to mechanical usage (SATMU): 4. Mechanical influences on intact fibrous tissues. Anat Rec 1990, 226(4):433-439.
19. Pattin CA, Caler WE, Carter DR: Cyclic mechanical property degradation during fatigue loading of cortical bone. J Biomech 1996, 29(1):69-79.

Original Article

Comparison of Peri-Implant Bone Stress with Different Implant Crest Module Designed by 3D Finite Element Analysis

Hsin-Mei Hsieh
Department of Stomatology, Veterans General Hospital, Taipei.
School of Dentistry, National Yang-Ming University, Taiwan.

Ming-Lun Hsu
Professor and Dean
School of Dentistry
National Yang-Ming University

Mail: mlhsu@ym.edu.tw
Tel: +886-2-28212943
Fax: +886-2-28264053

DOI: 10.6926/JPI.201812_7(4).0005

Abstract

Purpose: The mechanism of early implant bone loss is not fully understood, and there is ongoing controversy regarding which implant crest module geometry is more favorable for the preservation of crestal cortical bone. The main purpose of this study was to compare the stress placed on crestal cortical bone by three different types of implant crest module designs: divergent, straight, and convergent designs.

Material and methods: Models of divergent, straight, and convergent implant crest modules including an implant body, prostheses, and portion of the posterior left mandible were fabricated. To simulate osseointegration, the models were designed as if "bonding" had occurred between the implant and alveolar bone. A vertical loading of 200 N was applied over five occlusal contacts to simulate the maximum intercuspal position. An oblique loading of 200 N was applied at two occlusal contacts over the buccal cusps at a 30-degree angle with the direction of buccal to lingual. The stress distribution in the peri-implant bone and the displacement of the implant were then analyzed.

Results: The peak von Mises stress was concentrated around the crestal region of the cortical bone and the bottom of the cortical bone, especially in the convergent model. The maximal von Mises stress values of the divergent, straight, and convergent models were 41.4 MPa, 54.3 MPa, and 62.4 MPa, respectively, during vertical loading and 88 MPa, 90.6 MPa, and 112.6 MPa, respectively, during oblique loading.

Conclusion: Under the limitations of this study, the convergent implant crest module model induced more stress concentrated around the cortical bone and implant crest module area, especially in the oblique loading condition. The shape of an implant crest module may thus play an important role in the stress distribution around bone.

Key words: early implant bone loss, implant crest module, stress distribution, finite element analysis

Introduction

To date, the survival rate of dental implants is about 91~100%, and the success rate is about 84~97%. The most commonly used criterion for implant success, which was proposed by Albrektsson et al.[1] and Smith and Zarb[2], is a marginal bone loss of less than

1.5 mm for the first year and 0.2 mm for each subsequent year, However, the mechanism underlying a marginal bone loss of 1.5 mm or more in the first year is not yet fully understood.

According to the definition proposed by Adell et al.[3], early implant bone loss consists of the marginal bone loss resulting from the combined effects of implant placement and implant loading within the first year. Although the mechanism of early implant bone loss is not fully understood, it has been postulated that a number of factors may influence this process[4], including surgical trauma, microgaps, biologic width, occlusal overload, and the design of the implant crest module. Also, some studies have suggested that stress concentrated at the junction of the implant crest module and crestal cortical bone is related to marginal bone loss[4]. Early implant bone loss is related not only to functional but also esthetic complications, and the esthetic outcomes of implant restoration are regarded as increasingly important nowadays. In any case, it seems likely that implant design and the load distribution at the implant-bone interface play an important role in early implant bone loss, and so these factors should be considered in searching for solutions to prevent or decrease the amount of early implant bone loss.

To prevent or decrease the amount of early implant bone loss, implant manufacturers have modified both the macro- and micro-structures of implants. However, there is ongoing controversy regarding which implant crest module geometry is more favorable for the preservation of crestal cortical bone. There are three types of implant crest module geometries now commercially available: divergent, straight, and convergent (Fig. 1). There is still no consensus, however, as to which kind of implant crest module shape is more favorable for limiting crestal bone loss. The main purpose of this study, therefore, was to compare the stress placed on crestal cortical bone by divergent, straight, and convergent implant crest module designs.

Material and methods

The ANSYS Workbench 15 (ANSYS, Pennsylvania, United States) was used to construct the posterior mandible region. Each bone block used was approximately 12 mm in width bucco-lingually, 27 mm in height inferior-superiorly, and 20 mm in length mesial-distally. Each bone block consisted of cancellous bone surrounded by 1.5 mm thick cortical bone[5](Fig. 2). The length of each implant body was 10 mm, including the 1.5 mm of implant crest module. The coronal part of each implant at bone level was different in order to compare divergent, straight, and convergent shape designs of the implant crest module. The width of the divergent model was 5 mm, the width of the straight model was 4 mm, and the width of the convergent model was 3 mm (Fig. 3). Meanwhile, the diameter below the implant crest module was 4 mm for all the models. The implant thread design had a 0.33 x 0.33 mm square shape with a 0.8 mm screw pitch[6]. The height of the implant abutment was 7 mm with a core area of 5 mm in height for the crown-retained portion[7], while the dimension of the core was 4 mm in the coronal area, the diameter of the abutment was 7.7 mm, and the shoulder margin was 0.5 mm. For simplicity, the implant abutment and implant body were set as a one-piece unit. For implant restoration, a D800 dental laboratory scanner (3Shape, Copenhagen, Denmark) was used to scan a lower left first molar typodont tooth. After that, the typodont image data and implant data were input into Meshmixer 3.2 (Autodesk, California, United States) and combined in order to construct the crown portion. The crown was 11.85 mm in length and 10.55 mm in width. The maximum crown thickness was 2.82 mm. In order to transfer the data to the solid body, FreeCAD 0.16 (Free Software Foundation, Massachusetts, United States) was used to convert the data to the form of a STEP file. Finally, we input the crown portion data into ANSYS Workbench 15 and analyzed the stress distribution.

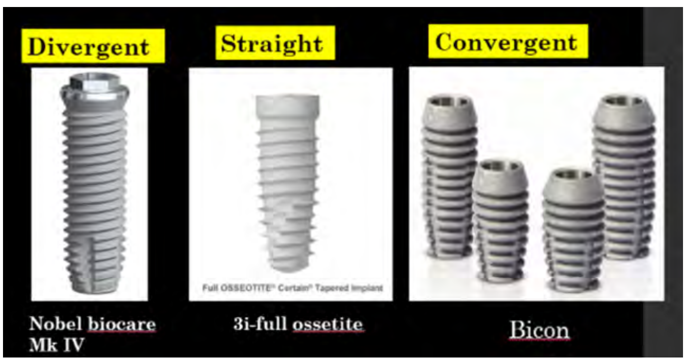

Fig. 1: Three types of implant crest module geometries which are commercially available: divergent, straight and convergent.

Bone is anisotropic in nature[5, 8, 9]. We therefore assumed that the bone was an anisotropic material. The material properties are shown in Table I. The material properties of the crown[10] and implant[11] were assumed to be isotropic, homogeneous, and linearly elastic, and the material properties are shown in Table II. The interface between the bone and implant was set as "bonded" to simulate the stage after socket healing and perfect implant osseointegration. The crown and implant interface were set as bonded without any loosening, while the cement space was neglected[12]. Two types of loading condition were used: axial loading and oblique loading. The axial loading was used to simulate the conditions of the maximum intercuspal position[13,14]. The loading was applied over five occlusal contacts of the lower first molar, including the cusp tip, the crest of the marginal ridge, and the bottoms of the fossae. According to a study by Sultana et al.[15], the average occlusal contact area of the lower first molar is 2.5 mm^2. To simplify the occlusal contact, we assumed the contact areas to be round in shape, with the radius of each being about 0.4 mm. We then used this information to create five occlusal contacts with Meshmixer 3.2 (Fig. 4). For the oblique loading condition, two of the five occlusal contacts of the maximum intercuspal position at the buccal cusp were used to simulate the grinding phase when chewing (Fig. 4). The angulation of the loading force was 30 degrees between the force and the long axis of the tooth, with the direction being buccal to lingual[13, 16].The force applied in both loading conditions was 200 N in order to simulate normal chewing force[17]. For the vertical loading, the force applied to each of the five occlusal contacts was set at 40 N. For the oblique loading, two of the occlusal contacts were chosen, and the force applied to each occlusal contact was set at 100 N and applied at a 30-degree angle with the direction of buccal to lingual. The 200 N of force used in the ANSYS Workbench 15 was "remote force", which is used as an alternative way to apply force to the body. The workbench calculates the equivalent moment and force and applies them to the body. The mesial and distal end of the mandible were set to "fixed support", so that the displacement of nodes in these directions was equal to zero[18].

Results

The number of elements and nodes are shown in Table III.

During vertical loading, the peak von Mises stress was concentrated around the crestal region of the cortical bone and the bottom of the cortical bone, especially in the convergent model. In terms of the occlusal view, the von Mises stress was concentrated on the buccal and lingual area. The maximal von Mises stress values of the divergent, straight, and convergent models were 41.4 MPa, 54.3 MPa, and 62.4 MPa, respectively (Fig. 5).

During oblique loading, the peak von Mises stress was mostly concentrated on the crestal region of the cortical bone and only partially concentrated on the bottom of the cortical bone. In terms of the occlusal view, the von Mises stress was concentrated only on the lingual area. The maximal

Table I

Material properties of cortical and cancellous bone

Material	Young's modulus (MPa)	Poisson's ratio (ν)	Shear modulus (MPa)	Reference
Cortical bone	Ex=17900	ν_{xy}=0.18	G_{xy}=4500	5, 8, 20
	Ey=12500	ν_{yz}=0.31	G_{yz}=5300	
	Ez=26600	ν_{xz}=0.28	G_{xz}=7100	
Cancellous bone	Ex=1148	ν_{xy}=0.055	G_{xy}=68	
	Ey=210	ν_{yz}=0.055	G_{yz}=68	
	Ez=1148	ν_{xz}=0.322	G_{xz}=434	

The x-direction is mesial-lateral, the y-direction is inferio-superior, and the z-direction is anterioe-posterior von Mises stress values of the divergent, straight, and convergent models were 88 MPa, 90.6 MPa, and 112.6 MPa, respectively (Fig. 6).

During vertical loading, the peak von Mises stress of the implant was concentrated on the first thread. The maximal von Mises stress values of the divergent, straight, and convergent implants were 47.5 MPa, 69.1 MPa, and 66.3 MPa, respectively (Fig. 7).

During oblique loading, the peak von Mises stress of the divergent implant was concentrated on the junction between the implant crest module and the implant body. The von Mises stresses of the straight and convergent models were concentrated on the lingual side of the implant crest modules. The maximal von Mises stress values of the divergent, straight, and convergent implants were 94.9 MPa, 127.1 MPa, and 298.2 MPa, respectively (Fig. 8).

During vertical loading, the maximal displacement values of the divergent, straight, and convergent models were 13.7 μm, 15 μm, and 16 μm, respectively, and during oblique loading, the maximal displacement values of the divergent, straight, and convergent models were 31 μm, 37.7 μm, and 51.4 μm, respectively.

Discussion

The results favored the divergent implant crest module, which showed the least stress concentrated on the crestal cortical bone area. Meanwhile, the convergent implant crest module showed the greatest stress concentration.

The first possible reason for these results was the total surface area of each implant crest module. The total surface area of the divergent implant crest module was greater than those of the straight and convergent designs, and when the total surface area is wider, the stress will be distributed more evenly.

The second possible reason for the results was the rigidity of the implant body. Wide diameter implants show less displacement. During vertical loading, the maximal displacement values of the divergent, straight, and convergent models were 13.7 μm, 15 μm, and 16 μm, respectively. The convergent model showed the greatest displacement, which indicates that lower rigidity may have contributed to this result, which would, in turn, eventually cause more stress to be induced at the bone-implant interface. This differences in

Table II

Material properties of implant and crown

Material	Young's modulus (MPa)	Poisson's ratio (ν)	Reference
Implant/abutment (CP Ti grade 4)	102000	0.3	11
Crown (gold alloy)	90000	0.3	10

Table III

The number of elements and node

	Elements	Nodes
Divergent model	100750	170670
Straight model	99925	169251
Convergent model	100645	170543

displacement were even more obvious under the oblique loading condition. During oblique loading, the maximal displacement values of the divergent, straight, and convergent models were 31 μm, 37.7 μm, and 51.4 μm, respetively.

The third possible reason for the results was the geometry of the cortical bone. When the implant crest module is divergent, there is a blunt angle at the top of the cortical bone; when the implant crest module is straight, there is a right angle at the top of the cortical bone; and when the implant crest module is convergent, there is an acute angle at the top of the cortical bone. An acute angle at the top of the cortical bone would induce greater stress concentration than a blunt angle.

Bone is anisotropic in nature[5, 8, 9], which means that its mechanical properties are different when measured in different directions in the same sample. However, a lot of studies have assumed bone to be an isotropic material in their finite element models[19], when in fact, the stress and strain levels in anisotropic bone are higher than those in isotropic bone[20]. In our study, we tried to use models that were close to the reality, so we assumed that bone is an anisotropic material. In order to compare the different implant crest module designs, gold alloy restoration was selected due to its ductile property, which meant that the stress could be more evenly distributed when loading was applied. Because we focused on the stress and strain over the cortical bone area, the cement space could be neglected[12].

The maximal biting force varies from individual to individual, ranging from 8 N ~ 880 N[21]. The average chewing force of an implant restoration is about 200 N at the first molar area [53, 72]. According to a literature review, it appears that most finite element analyses have assumed that occlusal loads are directly applied on the abutment of dental implants[22]. Such studies failed to consider the effect of a prosthetic crown in the clinical setting. The application of a load on a crown or implant leads to different bending moments[23]. Therefore, in our study, we scanned the morphology of a lower left first molar typodont tooth as our implant prosthesis model. Compared to other studies[24], therefore, the morphology of the prostheses used in this study was more close to that of clinical situations. According to Eskitascioglu et al.[25], the location of loading influences the stress distribution. We simulated the maximal intercuspal position as the vertical loading. It is the reason why, when cusp tips contact flat surfaces, the resultant force is directed vertically through the long axis of the teeth[13]. According to optimal occlusion[13, 14], we set up five occlusal contacts in our models. Under oblique loading, the tooth contact during mastication can be divided into the crushing phase and the grinding phase. In the crushing phase, the buccal cusps of the mandibular teeth are almost directly under the buccal cusps of the maxillary teeth. After that, the mandible's movement continues to close the bolus of food between the teeth, which begins the grinding phase. During the grinding phase, the mandible is guided by the occlusal surface of the teeth and moves back to the maximum intercuspal position, which causes the cuspal inclines of the teeth to pass across each other, permitting shearing and grinding of the bolus of food[13]. Therefore, the angulation of the force depends on the inner inclination of the maxillary cusp[16]. The angulation between the force direction and the long axis of the tooth was set to be 30 degrees in this study. Under the oblique loading condition, two occlusal contacts on the buccal cusp of the lower first molar were selected, and the direction of the reaction force was from buccal to lingual[13].

The limitations of this study were as follows: (1) the diameter of the abutment was not constant due to the different implant crest module designs; (2) the same total area with different contours might need to be tested; and (3) the finite element analysis could be applied for mechanical properties, but the relevant biological properties should be confirmed clinically.

Conclusion

Under the limitations of this study, the convergent implant crest module model induced more stress concentrated around the cortical bone and implant crest module area, especially in the oblique loading condition. The shape of an implant crest module may thus play an important role in the stress distribution around the bone.

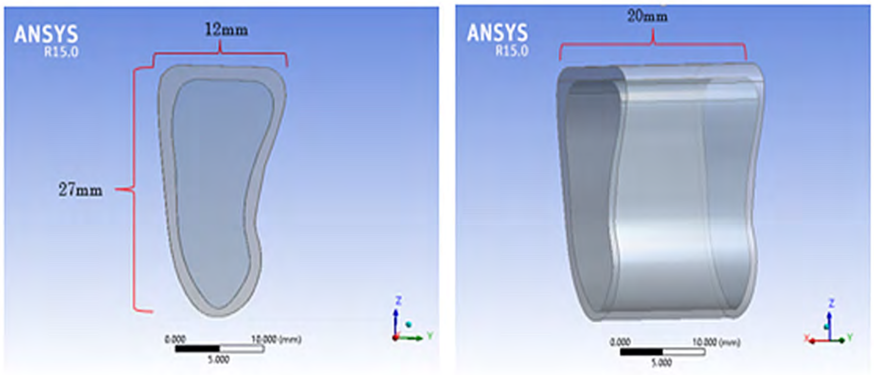

Fig. 2: Bone block : the bone block is approximately 12mm in width bucco-lingually, 27mm in height inferio-superiorly, and 20mm in length mesial-distally. The bone block is consisted of cancellous bone surrounded by 1.5mm thickness of cortical bone.

Fig. 3: The implant body with different implant crest module geometries, from top to down: divergent, straight, and convergent; the diameters of implant platform, from top to down, 5mm, 4mm, 3mm.

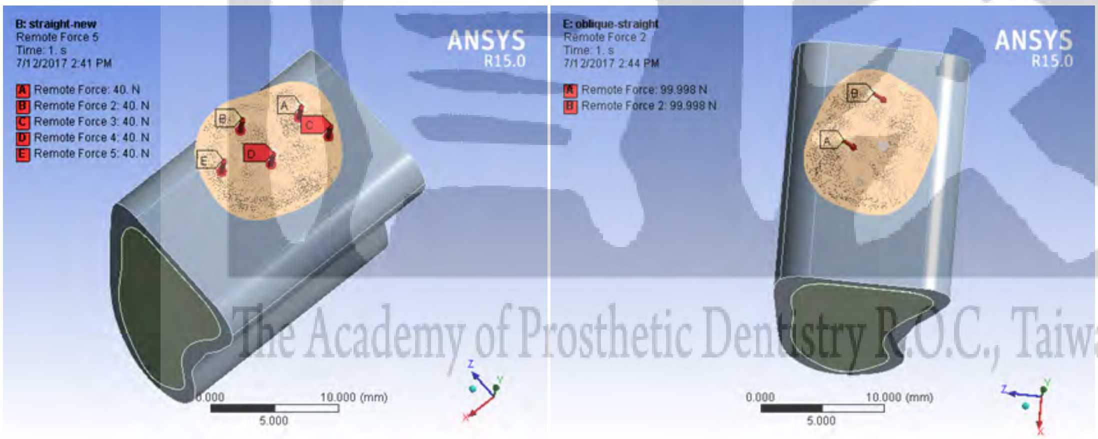

Fig. 4: (left) Under vertical loading, each of the five occlusal contacts was set to be 40 N (right) Each occlusal contact was set to be 100N at 30 degrees with the long axis of the tooth from buccal to lingual.

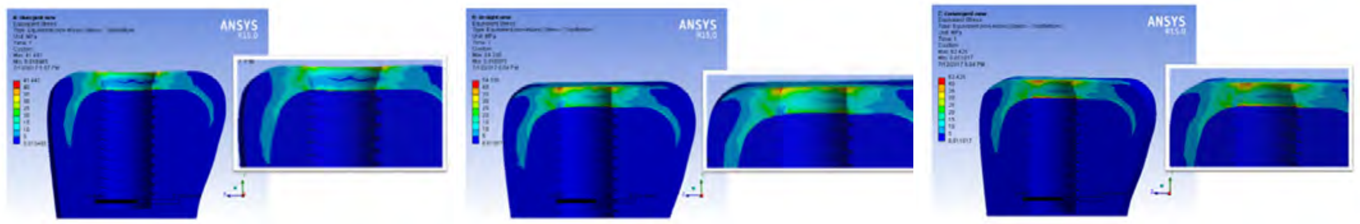

Fig. 5: Under vertical loading condition: distribution of von Mises stress around bone(MPa).

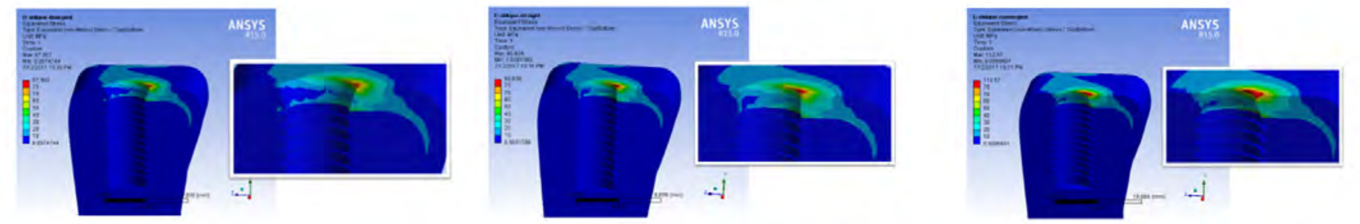

Fig. 6: Under oblique loading condition: distribution of von Mises stress around bone(MPa).

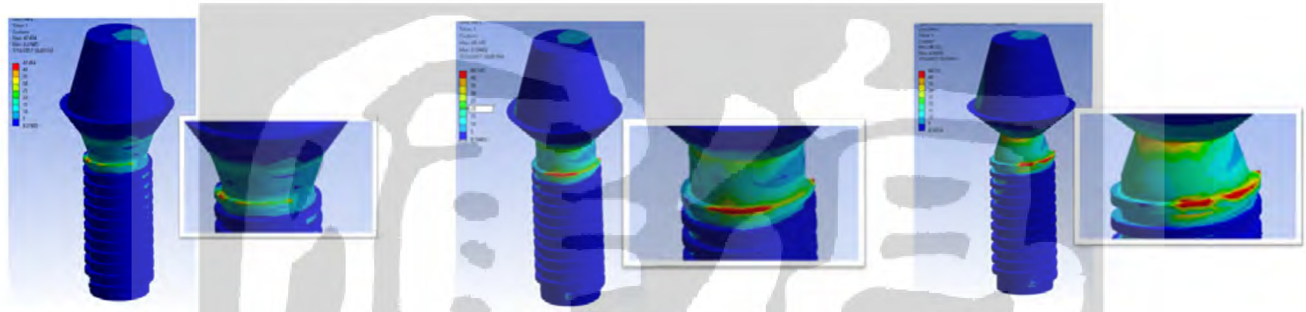

Fig. 7: Under vertical loading condition: distribution of von Mises stress of implant.

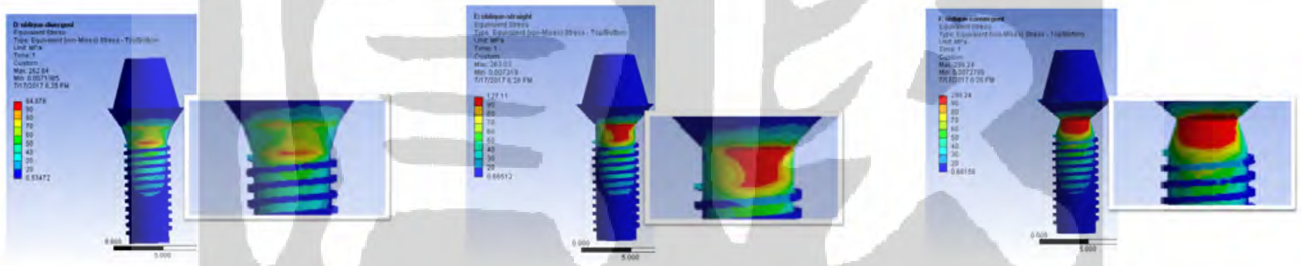

Fig. 8: Under oblique loading condition: distribution of von Mises stress.

References

1. Albrektsson, T., et al., The long-term efficacy of currently used dental implants: a review and proposed criteria of success. Int J Oral Maxillofac Implants, 1986. 1(1): p. 11-25.
2. Smith, D.E. and G.A. Zarb, Criteria for success of osseointegrated endosseous implants. J Prosthet Dent, 1989. 62(5): p. 567-72.
3. Adell, R., et al., A 15-year study of osseointegrated implants in the treatment of the edentulous jaw. Int J Oral Surg, 1981. 10(6): p. 387-416.
4. Oh, T.J., et al., The causes of early implant bone loss: myth or science? J Periodontol, 2002. 73(3): p. 322-33.
5. Schwartz-Dabney, C.L. and P.C. Dechow, Edentulation alters material properties of cortical bone in the human mandible. J Dent Res, 2002. 81(9): p. 613-7.
6. Chang, P.K., et al., Distribution of micromotion in implants and alveolar bone with different thread profiles in immediate loading: a finite element study. Int J Oral Maxillofac Implants, 2012. 27(6): p. e96-101.
7. Misch, C.E., Dental Implant Prosthetics. 2nd ed. 2014: Elsevier Health Sciences.
8. Dechow, P.C., Q. Wang, and J. Peterson, Edentulation alters material properties of cortical bone in the human craniofacial skeleton: functional implications for craniofacial structure in primate evolution. Anat Rec (Hoboken), 2010. 293(4): p. 618-29.
9. O'Mahony, A.M., et al., Anisotropic elastic properties of cancellous bone from a human edentulous mandible. Clin Oral Implants Res, 2000. 11(5): p. 415-21.
10. Benzing, U.R., H. Gall, and H. Weber, Biomechanical aspects of two different implant-prosthetic concepts for edentulous maxillae. Int J Oral Maxillofac Implants, 1995. 10(2): p. 188-98.
11. Tada, S., et al., Influence of implant design and bone quality on stress/strain distribution in bone around implants: a 3-dimensional finite element analysis. Int J Oral Maxillofac Implants, 2003. 18(3): p. 357-68.
12. Proos, K.A., et al., Influence of cement on a restored crown of a first premolar using finite element analysis. Int J Prosthodont, 2003. 16(1): p. 82-90.
13. Okeson, J.P., Management of Temporomandibular Disorders and Occlusion. 2014: Elsevier Health Sciences.
14. Nelson, S.J., Wheeler's Dental Anatomy, Physiology and Occlusion. 2014: Elsevier Health Sciences.
15. Sultana, M.H., K. Yamada, and K. Hanada, Changes in occlusal force and occlusal contact area after active orthodontic treatment: a pilot study using pressure-sensitive sheets. J Oral Rehabil, 2002. 29(5): p. 484-91.
16. Preis, V., et al., Influence of cusp inclination and curvature on the in vitro failure and fracture resistance of veneered zirconia crowns. Clin Oral Investig, 2014. 18(3): p. 891-900.
17. Ferrario, V.F., et al., Single tooth bite forces in healthy young adults. J Oral Rehabil, 2004. 31(1): p. 18-22.
18. Himmlova, L., et al., Influence of implant length and diameter on stress distribution: a finite element analysis. J Prosthet Dent, 2004. 91(1): p. 20-5.
19. Ramos Verri, F., et al., Biomechanical influence of crown-to-implant ratio on stress distribution over internal hexagon short implant: 3-D finite element analysis with statistical test. J Biomech, 2015. 48(1): p. 138-45.
20. O'Mahony, A.M., J.L. Williams, and P. Spencer, Anisotropic elasticity of cortical and cancellous bone in the posterior mandible increases peri-implant stress and strain under oblique loading. Clin Oral Implants Res, 2001. 12(6): p. 648-57.
21. Bates, J.F., G.D. Stafford, and A. Harrison, Masticatory function - a review of the literature. III. Masticatory performance and efficiency. J Oral Rehabil, 1976. 3(1): p. 57-67.
22. Yamanishi, Y., et al., Influences of implant neck design and implant–abutment joint type on peri-implant bone stress and abutment micromovement: Three-dimensional finite element analysis. Dental materials, 2012. 28(11): p. 1126-1133.
23. Falcon-Antenucci, R.M., et al., Influence of cusp inclination on stress distribution in implant-supported prostheses. A three-dimensional finite element analysis. J Prosthodont, 2010. 19(5): p. 381-6.
24. Chang, C.L., C.S. Chen, and M.L. Hsu, Biomechanical effect of platform switching in implant dentistry: a three-dimensional finite element analysis. Int J Oral Maxillofac Implants, 2010. 25(2): p. 295-304.
25. Eskitascioglu, G., et al., The influence of occlusal loading location on stresses transferred to implant-supported prostheses and supporting bone: A three-dimensional finite element study. J Prosthet Dent, 2004. 91(2): p. 144-50.

Introductions for authors

The Journal of Prosthodontics and Implantology is an official publication of the Academy of Prosthetic Dentistry, R.O.C., published quarterly in April, July, November and January. Articles related to clinical and basic prosthodontics, implantology, implant related periodontology, periodontology and surgery as well as biological and material sciences related to prosthodontics ad implantology are welcome. Articles may be categorized as original paper, case report, technical reports and literature review related to future research. Invited review articles are written by representative scholars on some important topics this journal wishes to emphasize.

Submitted papers will be evaluated by the editorial board and invited reviewers. Papers submitted shall not be accepted or published by any other journals. Papers published in this journal will become the copyright of this journal and shall not be subsequently published in any other publication in any language without prior written consent of the publisher.

Manuscript should be prepared according to the guidelines produced by the International Committee of Medical Journal Editors: Uniform Requirements for Manuscripts submitted to Biomedical Journals. Further information can be found at http://www.icmje.org.

Manuscript should be submitted via e-mail at the address of: prosthor@ms48.hinet.net

The manuscript format

1. Title page: including title, names and institutions of each author. Corresponding author should also provide mailing address, phone and fax number and e-mail address. A running title no more than 40 words and no more than 4 keywords should also be provided.
2. Abstract: no more than 400 words, should briefly describe the purposes of the study, material and methods used, results and discussion with conclusion.
3. Text:
   A. Review articles: can be of author's preferred format.
   B. Original articles: should include introduction, materials and methods, results, discussion and conclusion.
   C. Case reports and technical reports: should include introduction, case or technique description and discussion.
4. References: All publications cited in the text should be presented in the references part. The order of references should follow the order cited in the text. Examples of the reference style of this journal are as follow:
   A. Journal reference style: List all authors if the number is six or less. If the author number is more than six, list six authors and add et al for the remaining authors.
      (1) Journal article: Lin YT, Chang LC. Space changes after premature loss of the mandibular primary first molar: a longitudinal study. J Clin Pediatr Dent 1998; 22: 311-6.
      (2) Online journal article: Yavuz MS, Aras MH, Büyükkurt MC, Tozoglu S. Impacted mandibular canines. J Contemp Dent Pract 2007; 8: 78-85. Available at: http://www.thejedp.com/issue036/index.htm. Accessed November 20, 2007.
   B. Book reference style:
      (1) Complete book: McDonald RE, Avery DR. Dentistry for child and adolescent. 5th ed, Mosby Co, St Louis, 1988; pp339-41.
      (2) Chapter in book: Moore BK, Avery DR. Dental materials. In: McDonald RE, Avery DR (ed). Dentistry for child and adolescent. 6th ed., Mosby Co., St. Louis, 1994; pp349-72.
5. Tables and Fig.s: should be kept in minimum number. Fig.s should be in JPG, EPS or TIF file and can be e-mailed to the editor. They should be clear enough and listed in separated pages. Scale marker should be provided for magnification. All abbreviations shown on the table and Fig. should be explained in the legend.
   Photos of patients should be obscured for identification. Otherwise a patient's consent form should be provided.
6. Further information can be found at http://www.prosthod.org.tw/

投 稿 須 知

一、 本期刊為季刊，每年四、七、十及一月出刊，以英文刊出。

二、 凡與基礎或臨床補綴學、顳顎關節或咀嚼功能、人工植體相關、牙科補綴之技工學有關之著作，均為刊載之對象。接受的稿件類型共有下列五種，來稿請註明類型：

1. 社論(editorial)
2. 學術綜論(review article，限邀稿)
3. 研究論文(original article)
4. 病例報告(case report)
5. 技術報告(technical report)

三、 稿件撰寫一般格式:

1. 稿件必須是沒有刊出或將被接受刊於其他雜誌者。
2. 以英文投稿，文章內容以複行(double spacing) 繕打，字體大小12以上，其每邊邊緣至少須留2.5公分，不須任何格式編排。
3. 全文總頁數 (包括摘要、圖、表、參考文獻) 以八頁為限，必要時可增至十二頁。
4. 請以電子文件投稿，文書處理程式建議以IBM-Microsoft Word 為主。須標示使用程式、投稿題目、第一作者姓名，將電子文件 e-mail 至: prosthor@ms48.hinet.net。
5. 請同時附上致本誌主編簡短信函，表明投稿本誌之意願，並說明所有著者均曾過目並簽名同意。若為人體試驗須附人體試驗委員會之同意函。

四、 稿件內容詳細規格如下:

1. 首頁 (title page): 包括題目、作者姓名、服務單位、學歷；英文簡題(running title) 長度在四十個字以內；稿件主要負責者(corresponding author)之英文姓名與地址、電話、傳真、e-mail。
2. 摘要 (abstract): 以400字為限，簡潔說明並標示研究目的、方法、結果、主要結論或新發現。若為原始著作則須說明並標示，並需附關鍵詞(key words) 5 個以內。
3. 本文 (text)：
   - A. 學術綜論(review article)—無一定格式。
   - B. 原始著作(original article)—分前言、材料與方法、結果、討論、結論。
     - (1) 前言 (introduction)：簡要說明研究由來。
     - (2) 材料與方法 (material and methods) 敘述研究設計、對象、步驟。
     - (3) 結果 (results)：研究結果以文字、表格或插圖表示之。
     - (4) 討論 (discussion): 強調重要結果與論點，與前人論述作比較等。
     - (5) 結論 (conclusion): 結論要簡要明確。
   - C. 技術報告(technical report)—分前言、方法描述、討論。
   - D. 病例報告(case report)—分前言、病例描述、討論。

4. 參考文獻 (references)：以出現於本文中之先後順序用阿拉伯數字(上標)排列之，書寫方式請參考 Cumulated Index Medicus，內容含作者姓名(全部列出)、篇名、期刊名、年代、頁數。例如：(1) 期刊之書寫： Lin YT, Chang LC. Space changes after premature loss of the mandibular primary first molar: a longitudinal study. J Clin Pediatr Dent 1998; 22: 311-6. (2) 書籍之書寫：McDonald RE, Avery DR. Dentistry for child and adolescent. 6th ed., Mosby Co, St Louis, 1994; pp339-41. (3)有編輯者之書籍章節書寫：Moore BK, Avery DR. Dental materials. In: McDonald RE, Avery DR. Dentistry for child and adolescent. 6th ed., Mosby Co., St. Louis, 1994; pp349-72. (4)電子期刊之書寫：Yavuz MS, Aras MH, üyükkurt MC, Tozoglu S. Impacted mandibular canines. J Contemp Dent Pract 2007; 8:78-85. Available at: http://www.thejedp.com/issue036/index.htm. Accessed November 20, 2007.

5. 插圖與表格 (Fig.s and tables)：
   (1) 插圖請勿放置於本文中，圖與表之數量盡量少，也不要編排，應儲存於另外的檔案夾。影像圖檔應以JPG、EPS或 TIF 形式存檔。插圖以電子檔e-mail 傳送投稿。
   (2) 插圖之標題及詳細說明，須另頁複行繕打。顯微照像須以比例尺 (internal scale marker) 標明放大倍數。
   (3) 病人臉部照片須遮蓋眼睛至無法辨認是何人的程度，否則須附病人之書面同意書。
   (4) 繪圖軟體應使用如Photoshop、Photoimpact、Illustrator等。彩色或灰階圖形須掃瞄至300 DPI，線條圖形則須至1200 DPI，並請標明圖檔名稱及所使用軟硬體名稱。
   (5) 圖或表中出現之字母或符號，均需於註解中詳細解釋。

五、 投稿清單

(1) 致主編簡短信函。
(2) 提供稿件主要負責者之姓名與地址(英文)、電話、傳真、e-mail、所有作者之服務機構(英文) 。
(3) 附英文摘要(400字以內) ，研究論文的摘要應分研究目的、方法、結果、主要結論。
(4) 附英文關鍵詞(5個以內) ；附英文簡題(長度在40個字以內)。
(5) 確認所有參考文獻的格式、內容、引用順序皆完整無誤。
(6) 確認所有表格(標題、註腳)及插圖之標題及詳細說明，另紙複行繕打。
(7) 確認所有圖表皆符合格式。圖表皆儲存於另外的檔案夾，而未放置於本文中。
(8) 若為人體試驗須附人體試驗委員會之同意函。
(9) 全部作者同意簽名之證明函。

六、 稿件一經刊載，版權屬本誌所有；本誌文章皆已上載至DOI，將不另行提供抽印本。

The Academy of Prosthetic Dentistry R.O.C., Taiwan

Table of Contents

Editorial

Case Report

Original Article

ISSN 2304-541-8
9 772304 541008